Nucl. Phys. A141, 664 (1970).
[25]D. R. Thompson, Nucl. Phys. A154, 442 (1970). Our data have been used with our permission in this paper. Unfortunately, the cross-section data we supplied Professor Thompson were too large by a factor of approximately 0.6.
[26]B. F. Gibson, private communication.
[27]D. R. Thompson, Nucl. Phys. A143, 304 (1970).
[28]A. B. Volkov, Nucl. Phys. 74, 33 (1965).
[29]These curves were calculated by Dr. J. J. Murphy, II.
[30]A. N. Gorbunov and V. M. Spiridonov, Zh. Eksperim. i Teor. Fiz. 34, 862 (1958) [transl.: Soviet Phys.-JETP 7, 596 1958)].

PHYSICAL REVIEW C VOLUME 6, NUMBER 1 JULY 1972

Giant Resonances in C^{12}†

C. Brassard,* H. D. Shay, J. P. Coffin,‡ W. Scholz,§ and D. A. Bromley
A. W. Wright Nuclear Structure Laboratory, Yale University, New Haven, Connecticut 06520

(Received 15 November 1971)

Detailed measurements on the reaction $B^{11}(p,\gamma)C^{12}$ are reported in the incident proton energy range $14 \leq E_p \leq 22$ MeV. Previously reported absolute cross sections for this reaction have been found to be in question. Measurements have been made leading to the first (2^+) and third (3^-) states of C^{12} in addition to the ground state. No evidence has been found for the predicted resonance at $E_x = 35$ MeV, also reported in earlier experimental work. Detailed calculations based on the one-particle–one-hole model wave functions of Gillet and Vinh-Mau have been compared with the experimental data using a complete R-matrix formalism. Repetition of these calculations using pure j-j configurations yields comparable agreement. Evidence for the importance of many-particle–many-hole configurations in the radiative capture process has been found, particularly in the reaction leading to the first and third excited states, but also in the ground-state reaction data. The calculations are significant in the sense that no new parameters are introduced, nor are any significant approximations used which are not already in the model wave functions under test. The isospin mixing in C^{12} is found to be very small, if the new absolute (p,γ_0) cross section reported here is used; this is in marked contrast to earlier estimates of this mixing.

I. INTRODUCTION

The radiative capture of protons by B^{11} is one of the most extensively studied nuclear reactions[1-4]; however, reliable data were until recently limited to incident proton energies below 14 MeV (shortly after completion of the experiment reported herein, Kernel and Mason extended the measurements to 21 MeV). This continuing interest in the detailed study of the interaction of γ radiation with nuclear matter reflects the relative simplicity of nuclear processes involving electromagnetic radiation. The relative weakness of the electromagnetic forces and our detailed knowledge of them permit the direct testing of nuclear wave functions, with minimal additional approximations. Furthermore, detailed model wave functions of highly excited states reached in these studies have only recently become available; these wave functions can be tested directly in calculations directed toward reproduction of radiative capture experimental results in the appropriate energy region.

C^{12} constitutes an especially interesting compound nucleus for study through radiative capture reactions, since its widely spaced low-lying levels permit the resolution of the radiative transitions to the first four states,[5] as pictured in Fig. 1, and since extensive information is already available on the structure of the lower-lying excited-state wave functions. Such knowledge is essential to any detailed study of the higher levels. Only the transitions to the ground state and first excited state had been reported previously. In the studies to be reported herein we have measured angular distributions for the reaction B^{11}-$(p,\gamma)C^{12}$ in the range from 14- to 22-MeV incident proton energy for the γ_0, γ_1, and γ_3 transitions; the γ_2 transition to the 7.65-MeV state is weak, and only an upper limit was obtained for the corresponding cross section.

The theoretical interest in the radiative proton capture experiments lies in the fact that the capture cross sections can be calculated directly from the detailed wave functions of the nucleus, without additional assumptions concerning either the reaction mechanism or the structure of the

projectile. Gillet's 1p-1h wave functions[6,7] for highly excited states in C^{12} (for which the ground state of C^{12} is arbitrarily taken as the vacuum) have been available for some time, and it was of interest to investigate their validity. Two major questions concerning these wave functions remained open. The first question concerns the advantage of introducing a residual interaction which mixes the 1p-1h configurations, and the second concerns the validity of the assumption of the purity of the 1p-1h states involved.

The results presented herein suggest that in C^{12} the wave functions are not improved by introducing a residual interaction which mixes the 1p-1h configurations. Many-particle–many-hole configurations are clearly evident, and the 1p-1h configurations appear to mix with them in preference to mixing with one another. Nevertheless, in the case of the ground-state transition, the 1p-1h model is relatively successful in predicting the angular distributions, simply because the γ_0 electric dipole decay must necessarily proceed through 1p-1h configurations. The situation is strikingly different for the γ_1 and γ_3 transitions, which cannot be accounted for in terms of the deexcitation of 1p-1h excitations.

Although otherwise consistent with our results, the work of Reay, Hintz, and Lee (RHL),[2] suggested the presence of a resonance at 35-MeV excitation in contradiction to our data; the resonance which they reported appears to have been purely a statistical phenomenon.

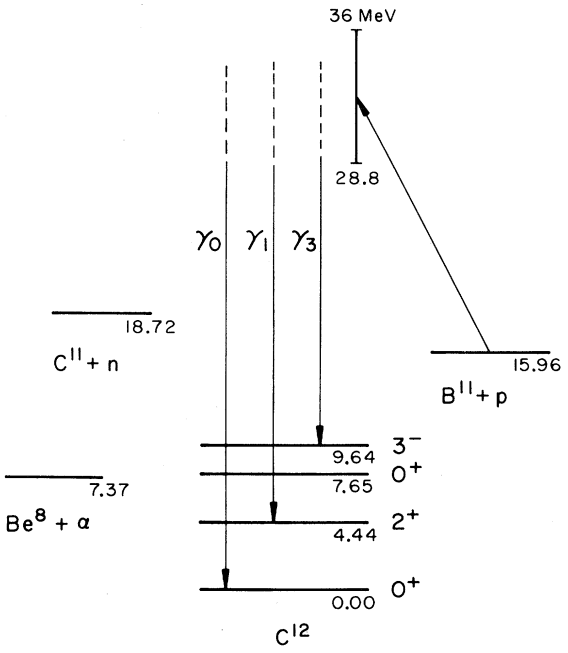

FIG. 1. The mass-12 energy-level diagram, showing the C^{12} ground state and first three excited states, and the neutron, the proton, and the α-particle thresholds. The three transitions reported herein and the energy range of the measurements are indicated.

It has been found that the previously reported absolute cross sections for the capture reaction $B^{11}(p,\gamma)C^{12}$ are in question; this has important consequences for earlier discussions of isospin mixing in C^{12} which were based on the relative magnitudes of (γ,n) and (γ,p) [actually (p,γ)] cross sections.

II. EXPERIMENTAL METHODS

The measurements were performed utilizing a proton beam from the Yale MP-1 tandem Van de Graaff accelerator; γ radiation was detected in a 9×12-in. NaI(Tl) crystal, and an on-line IBM 360/44 computer controlled the data-acquisition and data-analysis phases of the experiment. The angular distributions were obtained at each energy by moving the detector relative to the target.

Pulse Pileup

The most difficult experimental problem encountered was that of electronic pileup; in the worst conditions (i.e., at 22-MeV proton energy, at forward angles) only 1 in 10^8 counts in the crystal originated in the (p,γ) reactions of interest; the remaining counts also originated in the bombarded target but corresponded to the detection of neutrons or of cascading γ rays following particle emission. These produced an intense low-energy background in the γ-radiation spectrum. Such pile-up problems are typically solved by reducing the beam current until the total counting rate falls within the range of the electronic instrumentation in use. This procedure was not feasible in the experiment reported herein, however, because it would have resulted in (p,γ) rates lower than the underlying cosmic-radiation background in the detector. The NaI(Tl) crystal, on temporary loan from Oak Ridge National Laboratory,[8] pending completion of a Yale system, was not equipped with an anticoincidence shield.

The pile-up problem was solved through the design and construction of a fast electronic counting system, capable of counting up to 40 times faster than conventional double-delay-line amplifier systems. Brassard[9] has described this counting system which involves a compromise between resolution and counting rate but which does not involve the rejection of pileup[5] with its corresponding difficulties in determining both absolute and differential cross sections. Figure 2 shows a comparison of the performance of this fast counting system with that of a conventional double-delay-line pile-

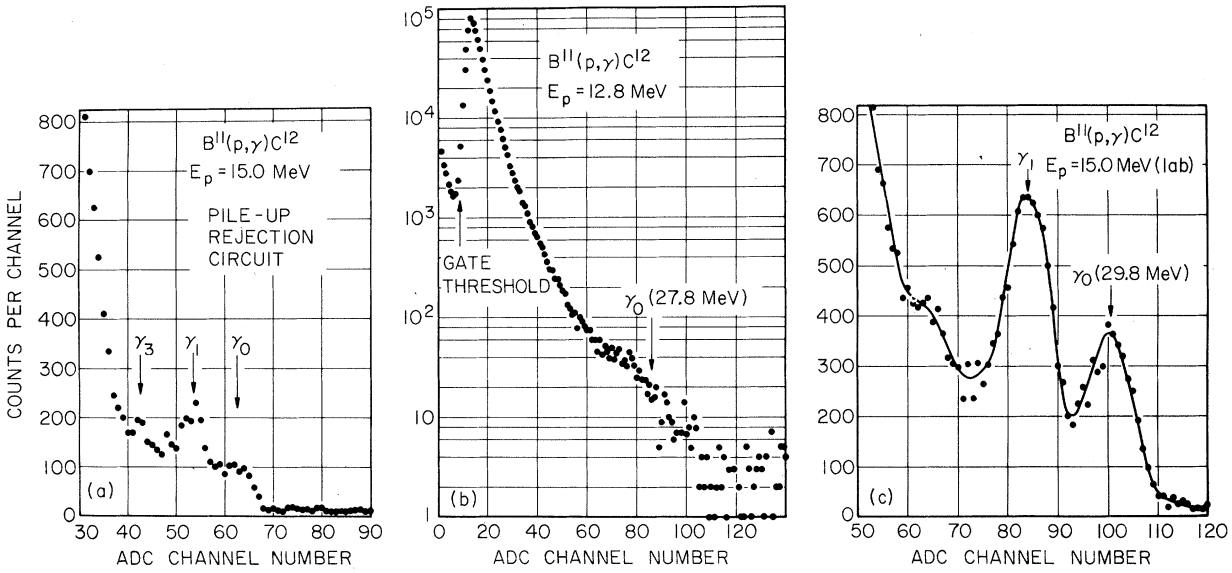

FIG. 2. Spectrum (a) was accumulated in 29 min using a conventional pile-up rejection circuit; when the counting rate is increased by a factor of 4, as in (b), many counts are rejected but the pileup nevertheless completely destroys the spectrum [the counting time for (b) was 10 min]. Spectrum (c) was obtained in 10 min with the fast counting system (Ref. 9) used at Yale.

up rejection circuit: Spectrum (a) was obtained in 20 min with the pile-up rejection circuit; in (b), the counting rate was increased by approximately a factor of 4, resulting in the complete destruction of the spectrum; (c) was accumulated in 10 min with our fast counting system. In all cases the target-detector geometry remained fixed.

Detector System

The detector used to measure the angular distributions reported herein was a 9×12-in. NaI(Tl) crystal, fitted with a 57 AVP 9-in. photomultiplier and shielded with 4000 lb of lead. The poor low-energy resolution of this detector (45% for Cs^{137}) was attributable to the low efficiency and other characteristics of this photomultiplier; however, the resolution for high-energy γ rays was adequate in the case of C^{12}.

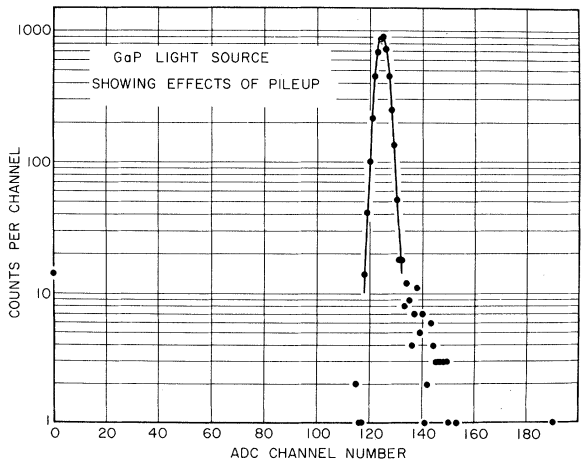

FIG. 3. Typical light-pulser spectrum used to monitor pileup and to permit on-line computer control of the photomultiplier gain. As seen by the asymetrical shape of the peak, pileup (counts above channel 135) always results in an increased pulse height.

A selected gallium phosphide light pulser was optically coupled to the photomultiplier, and the light-pulser spectrum was used both as a pile-up monitor and as a photomultiplier gain stabilizer. Figure 3 shows a typical light-pulser spectrum accumulated simultaneously with radiative capture events in the data-acquisition system. The tail on the right-hand side of the peak originates in pileup; no such tail is present on the left-hand side, because pileup in a completely direct-coupled counting system always results in an increased pulse height. The counts in channel zero correspond to the analog-to-digital converter dead time and form a convenient monitor of this dead time.

The light-pulser spectrum was automatically analyzed during the course of the measurements to determine the gain of the counting system and the severity of pileup. The photomultiplier gain was readjusted automatically, by the computer, to hold the centroid of the pulser peak fixed, and periodic reports on gain stability and pile-up conditions were printed out for permanent record. The measurements were performed at a characteristic 2% pile-up level; the light-pulser rate

was automatically adjusted to remain proportional to the incident proton beam current. Provision was made for automatic reduction of the beam current whenever the pileup detected through the broadening of the analyzed pulser peak exceeded preset limits.

Data Analysis

The resultant γ-radiation spectra were fitted using a special data-analysis program, based on the nonlinear least-squares-fit algorithm described by Brassard[5,10] which is extremely stable in fitting small peaks; the program was designed for on-line manipulation of spectra and directly yielded differential cross sections with their probable errors. The immediate availability of these results during the experiment permitted the optimization of the various conditions which prevailed during the data acquisition and enabled immediate decision-making concerning progress of the experiment and adequacy of the accumulated data.

Targets

The targets used for the angular-distribution measurements were made by mixing 99% isotopically enriched B^{11} powder with alcodag (a colloidal suspension of graphite in alcohol) and allowing a film of appropriate thickness of this mixture to dry *briefly* on a flat glass plate in air before immersing it in water for release from this substrate. Targets of reasonable homogeneity containing up to 80% B^{11} were produced by this method, in thicknesses ranging from 0.5 to 10 mg/cm^2. A 5-mg/cm^2 target was used in the experiment.

The carbon impurities could be tolerated because of the low Q value of the γ-ray producing reactions associated with carbon; however, the question of determining the exact B^{11} content of the target necessitated separate experiments to determine the absolute magnitude of the total cross sections. A description of these targets and methods adopted for these measurements are presented in the following section.

Absolute Cross-Section Determination

The absolute magnitudes of the total cross sections reported herein, not only of our higher-energy measurements, but also of our repetitions of previously available lower-energy data were obtained with an evaporated B^{11} target of gross thickness 244 μg/cm^2, whose areal density was established through measurement with an α-particle range gauge and whose composition was checked by measurements on several nuclear reactions of known cross sections.

One of the most basic experimental difficulties in the detection of high-energy γ radiation involves the determination of the response of the crystal to monoenergetic γ rays – i.e., the characteristic peak-shape determination. A reliable measurement of the peak shapes at the γ-radiation energies of interest here (15 to 36 MeV) is essentially impossible to obtain using nuclear-particle accelerators, because the high-energy γ rays of appropriate energy resulting from particle-induced nuclear reactions are always accompanied by an important, and usually unknown, low-energy radiation background. Typically, prior radiative capture studies[3] have adopted the use of response functions with sizable low-energy tails; these are peak shapes similar to those found in the studies of Kockum and Starfelt[11] with a 12.7-cm-diam by 20.4-cm NaI(Tl) crystal. More re-

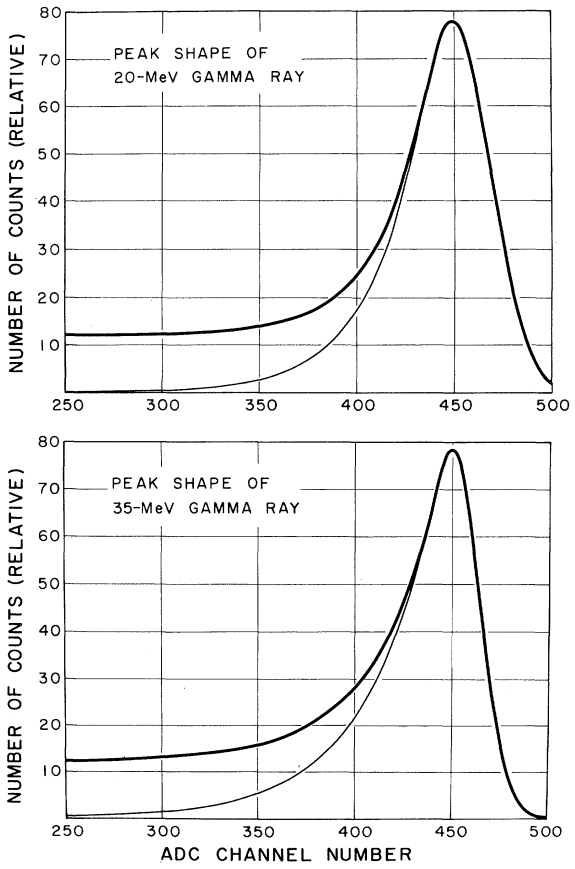

FIG. 4. Response of the 9× 12-in. NaI(Tl) detector system to monoenergetic γ radiation of 20 and 35 MeV, respectively. The area between the heavy line and the faint line originates in γ rays which were Compton-scattered in the paraffin shield which protected the crystal against fast neutrons emitted from the target.

cently, the Livermore photonuclear group[12] has carefully measured the response of a 20×20-cm crystal using monochromatic photons produced by the in-flight annihilation of positrons and tagged with the coincident detection of the second annihilation γ photon. At relatively low energies, e.g., 12.5 MeV, their results contrasted markedly with those of Kockum and Starfelt: The peak shape could be well fitted with a set of Gaussians (full-energy peak and escape peaks) smoothly joining exponentially decreasing low-energy tail, unlike the flat low-energy tail found by Kockum and Starfelt. These response functions varied little for either choice of collimators, 2.5 or 9.0 cm in diameter. At higher energies ($E_\gamma \leq 31.1$ MeV), the resolution of the 20×20-cm crystal worsened to roughly 11% because of escaping bremsstrahlung radiation [larger NaI(Tl) crystals typically exhibit full width at half maximum resolutions of 5–6%].[13] In the absence of peak shapes for large NaI crystals at high energy, the authors of this paper have elected to extrapolate from Livermore's 12.5-MeV peak shape by scaling the resolution by $(E_\gamma)^{-1/2}$. The faint lines of Fig. 4 show such peak shapes, with parameters adjusted for the particular detector used here. Direct measurement of peak shapes is not satisfactory, because of the low-energy neutron and γ background. Moreover, the detector system used in this radiative capture experiment is different from the arrangement used at Livermore, since it employs a paraffin shield interposed between the target and the detector, to shield the crystal from fast neutrons. The thickness of this paraffin shield is typically such that 50% of the incident γ rays undergo an interaction in it, and a corresponding correction (based on the tabulated cross sections for interaction of the γ ray in paraffin) must be used in determining the absolute cross sections. Because paraffin is a low-Z material, the dominant process is Compton scattering, and it would be expected that the Compton-scattered γ rays would produce a low-energy tail on the individual γ-ray peaks. This low-energy tail is in fact observed in any radiative capture reaction for which the first excited state of the residual nucleus lies at a high enough energy to permit a clear observation of the tail from the peak corresponding to the ground-state transition. A convenient example occurs in the reaction $N^{15}(p,\gamma)O^{16}$ which has been examined in this laboratory and elsewhere.[14] The simple paraffin-in, paraffin-out experiment is inconclusive because the great alteration in the neutron background obscures any changes in the low-energy tail.

The three basic detection processes which are displayed in Fig. 5. γ-ray number 1 did not interact in the paraffin and resulted in a full-energy count under the faint line of Fig. 4. γ-ray number 2 was Compton-scattered in the paraffin and results in a lower-energy count, in the tail of the observed peak. This γ ray, however, has already been taken into account in the paraffin absorption cross section and should not be counted again. γ-ray number 3 was not initially included in the solid angle subtended by the crystal collimator, but was scattered into it; it too should not be

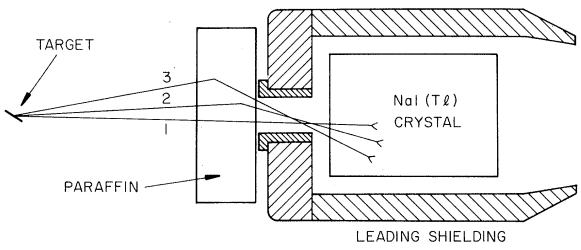

GEOMETRY OF A TYPICAL DETECTION SYSTEM FOR HIGH-ENERGY GAMMA RAYS

FIG. 5. This diagram shows three types of γ-ray events counted in the crystal: No. 1 is a normal count; No. 2 was included in the detector's solid angle, but was Compton-scattered by the paraffin; No. 3 was not included in the detector's solid angle initially, but was Compton-scatterd into it by the paraffin. Events of type 2 and 3 produce a low-energy tail on each peak of the γ-radiation spectrum.

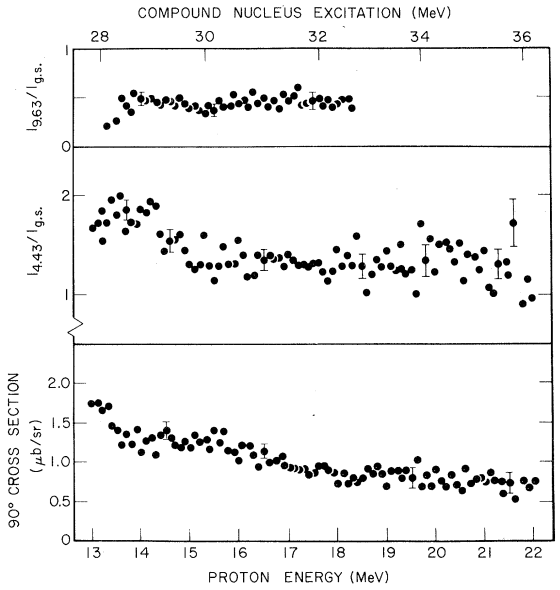

FIG. 6. Preliminary 90° results obtained with a 5×6-in. crystal. The γ_0 cross section is shown together with the branching ratios to the first and third excited states. The errors shown are only rough estimates, and the absolute magnitude of the total cross section has been determined by comparison with the thin-target yields.

counted as valid. The area between the faint and heavy lines of Fig. 4 is, therefore, interpreted as arising from Compton-scattered γ rays; the heavy line is used in fitting, whereas the faint line is used when obtaining absolute cross sections. This procedure appears well founded, but is not standard. In at least some of the previous work, the heavy line was extrapolated to zero and integrated under. This causes an important discrepancy in the experimental determination of the absolute magnitude of the total cross section in that the Compton-scattered component of the radiation from the paraffin absorber is incorrectly included. $B^{11}(p,\gamma_0)C^{12}$ cross sections measured both with and without 14 in. of paraffin moderator agree within errors, thus confirming at least the consistency of this fitting procedure. This choice of peak shapes, like any other, is, to some measure, arbitrary.

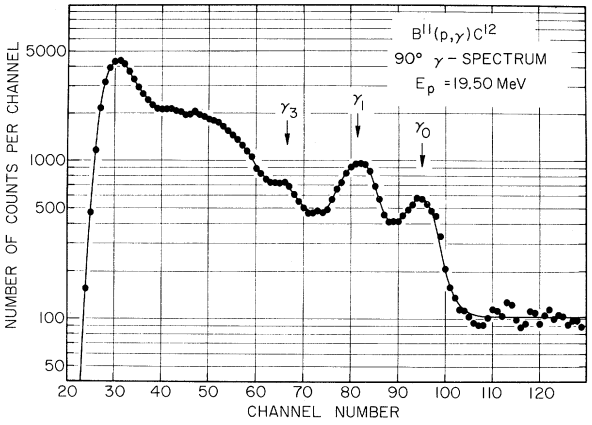

FIG. 7. Typical spectrum taken with the 9×12-in. NaI(Tl) crystal on loan from Oak Ridge and the Yale fast counting system.

III. EXPERIMENTAL RESULTS

The preliminary results shown in Fig. 6 were obtained at 90° with a smaller 5×6-in. crystal, in the energy region of 13- to 22-MeV incident proton energy; the energy increment was 200 keV. On the basis of the observed lack of fine structure in these measurements, the energy increment was increased to 500 keV in the subsequent, more complete, angular-distribution studies.

The differential cross sections for the reactions

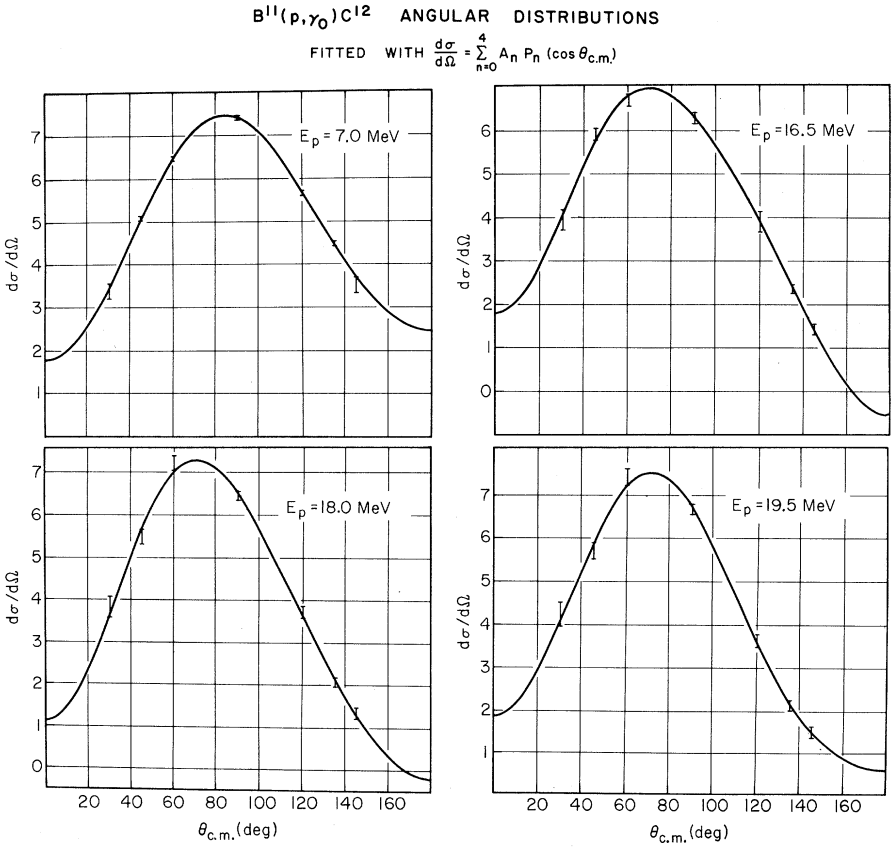

FIG. 8. Angular distributions of the γ_0 transition, in arbitrary units.

$B^{11}(p,\gamma)C^{12}$ were systematically measured at angles of 30, 45, 60, 90, 120, 135, and 145° in the energy range from 14 to 21 MeV. A typical γ-radiation energy spectrum is shown in Fig. 7, and typical angular distributions are given in Figs. 8–10.

The γ_0 and γ_1 angular-distribution results were fitted with a Legendre-polynomial expansion up to and including order four. The results are shown in Figs. 11 and 12; the A_1 to A_4 coefficients are defined by the expression:

$$\frac{d\sigma}{d\Omega} = \frac{\sigma_{\mathrm{TOT}}}{4\pi}\left[1+\sum_{K=1}^{4} A_K P_K(\cos\theta)\right].$$

On the basis of the χ^2 obtained in the least-squares-fitting procedure, the γ_3 angular distributions were fitted with P_0 and P_2 Legendre polynomials only, with the results shown in Fig. 13.

The transition to the second excited state of C^{12} was not observed, and it was possible to set an upper limit of 20% of the γ_1 cross section at any energy on it. No evidence has been found for the resonance which had been reported by RHL[2] at an excitation energy of 35 MeV.

In the case of the total cross sections, the errors shown have been obtained from complete inversion of the matrix of second derivatives, and all uncertainties of statistical origin are included; the errors shown with the angular-distribution coefficients A_1 to A_4, however, also include all statistical and systematic contributions, with the exception of the spectrum-fitting systematic error. The uncertainty in the target thickness and other possible systematic errors affecting the absolute value of the total cross sections are of the order of 20%. The spectrum-fitting systematic error is that introduced by fitting the spectra with an exponential low-energy background plus *ad hoc* peak shapes; this use of approximate peak and background shapes introduces this additional error which is difficult to evaluate. It is certainly a negligible contribution in the case of γ_0 and γ_1 which are well resolved; in the γ_3 case, however, we estimate that this peak-fitting systematic error could increase the quoted error by a factor of 1.5 at 14 MeV to a factor of 1.2 at 21 MeV, where the γ_3 peak is better resolved.

The γ_3 cross section does not vanish at a proton

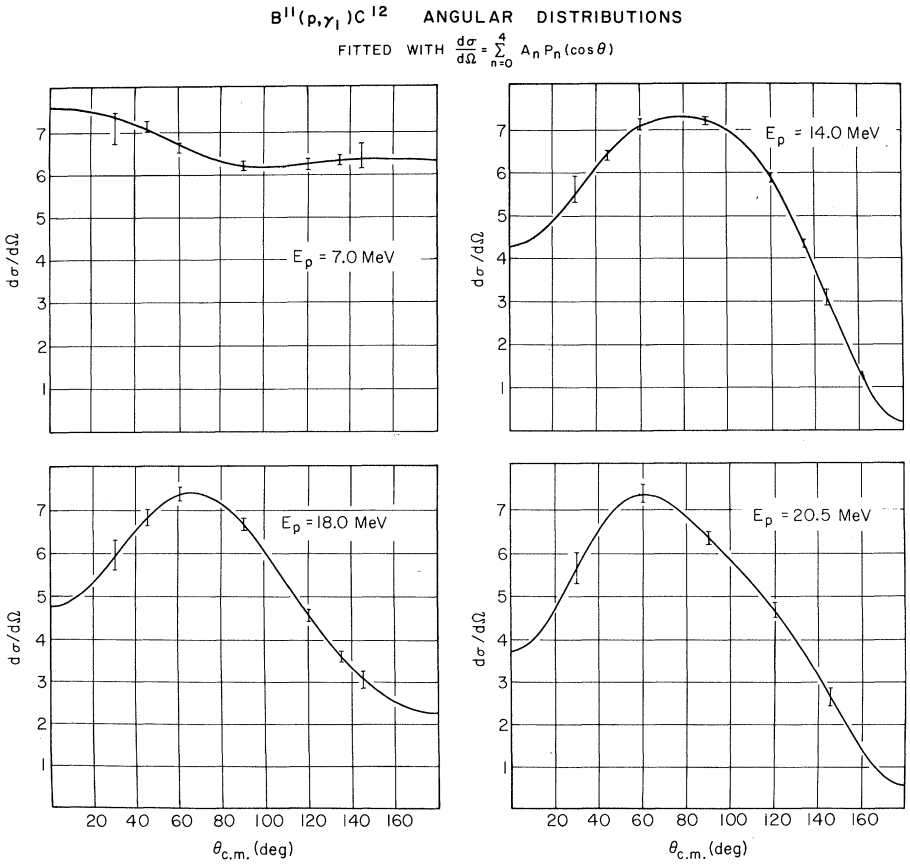

FIG. 9. Angular distributions of the γ_1 transition, in arbitrary units.

energy of 13 MeV, as our preliminary measurements had suggested; instead, the γ_3 peak disappears into the low-energy background, around E_p =11 MeV. This explains why this transition had not been reported in the earlier lower-energy measurements.

Figure 14 presents a comparison of the available experimental information on the (p,γ_0) cross section at 90° as reported by several authors. The results of Morrison[15] have been transformed from (γ,p_0) to (p,γ_0) using detailed-balance arguments. This agreement of the results so obtained with the work reported states of B^{11}, as can be surmised from the larger increments of bremsstrahlung end-point energies used in his experiment at these higher energies.

The careful work of Allas *et al.*[3] included angular-distribution measurements, not only to the ground state of C^{12}, but also to the first excited state. This work employed detector peak shapes with substantial low-energy tails. This is reflected in the fact that the Allas *et al.* cross sections, including γ_1 transition results, have been overestimated by the amount assumed under the tail. This correction is energy-dependent; fortunately, however, this energy dependence is slow enough that the correction factor of 0.61 applies with good accuracy throughout the energy range E_p=7 to 14 MeV.

The results of RHL[2] corroborate our findings, while those of Allas *et al.*[3] do not; this may merely reflect the fact that RHL used no paraffin shielding between the NaI(Tl) crystal and the target and, thus, did not observe the low-energy tail of Compton-scattered γ radiation.

IV. DISCUSSION OF RESULTS

Gillet and Vinh-Mau[6,7] have obtained a set of 1p-1h states in C^{12} based on configurations of two-major-shell excitations or less; calculations based on these wave functions have been compared with the present experimental results. The wave functions used are those of Gillet's "approximation 1"; they were obtained through diagonalization of a Hamiltonian with fitted residual interactions, in a truncated space of j-j coupled harmonic-oscillator single-particle states. The unperturbed energies were taken by Gillet from experiments on neighboring nuclei. Since the completion of this work,

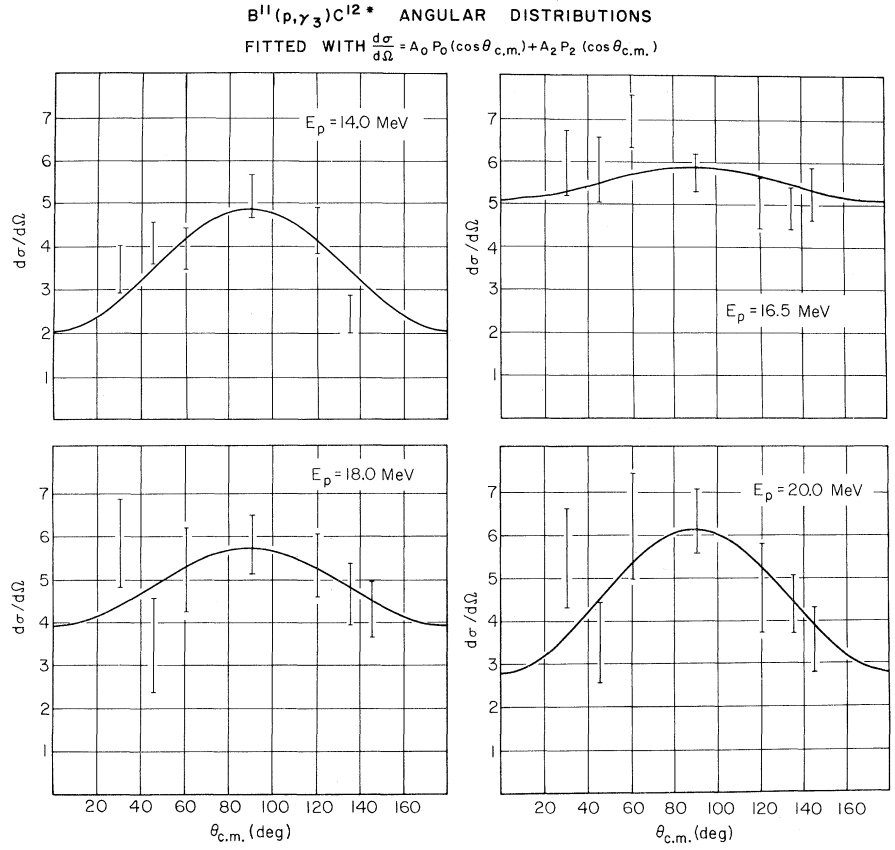

FIG. 10. Angular distributions of the γ_3 transition, in arbitrary units.

Wang, Shakin, and Feshbach[16] have shown that inclusion of three-particle–three-hole configurations neglected by Gillet and Vinh-Mau can result in important modifications of these predictions; measurements in this laboratory by Shay *et al.* on the reaction $Be^9(h,\gamma)C^{12}$, which will be published shortly, suggest that the 3p-3h excitations are indeed strong.

Calculation of Radiative Capture Cross Sections

Since in a particle-hole calculation, such as that of Gillet and Vinh-Mau, the average nuclear potential is conveniently approximated with an infinite harmonic-oscillator potential, the states and transitions are discrete. It has been customary to compare the experimental cross sections directly with the calculated intensities for the discrete transitions. This procedure, however, is only valid at relatively low excitation energies in the compound system, where the energy levels are far apart and give rise to isolated resonances. In the excitation region studied herein (see Fig. 1), a realistic $B^{11}(p,\gamma)C^{12}$ cross section must be calculated from the eigenstates of C^{12} before comparison with experiment can be considered meaningful.

This improved cross-section prediction may be obtained in various ways. Marangoni and Saruis,[17] for example, have obtained some ground-state results for C^{12}, in a coupled-channel framework, directly from the model Hamiltonian. It is also possible to interpret the stationary states of C^{12}, derived for an harmonic-oscillator potential, as valid approximations inside the nucleus, and to compute cross sections in the framework of R-matrix theory. This latter approach was exploited with limited success by Boeker and Jonker [18]; it

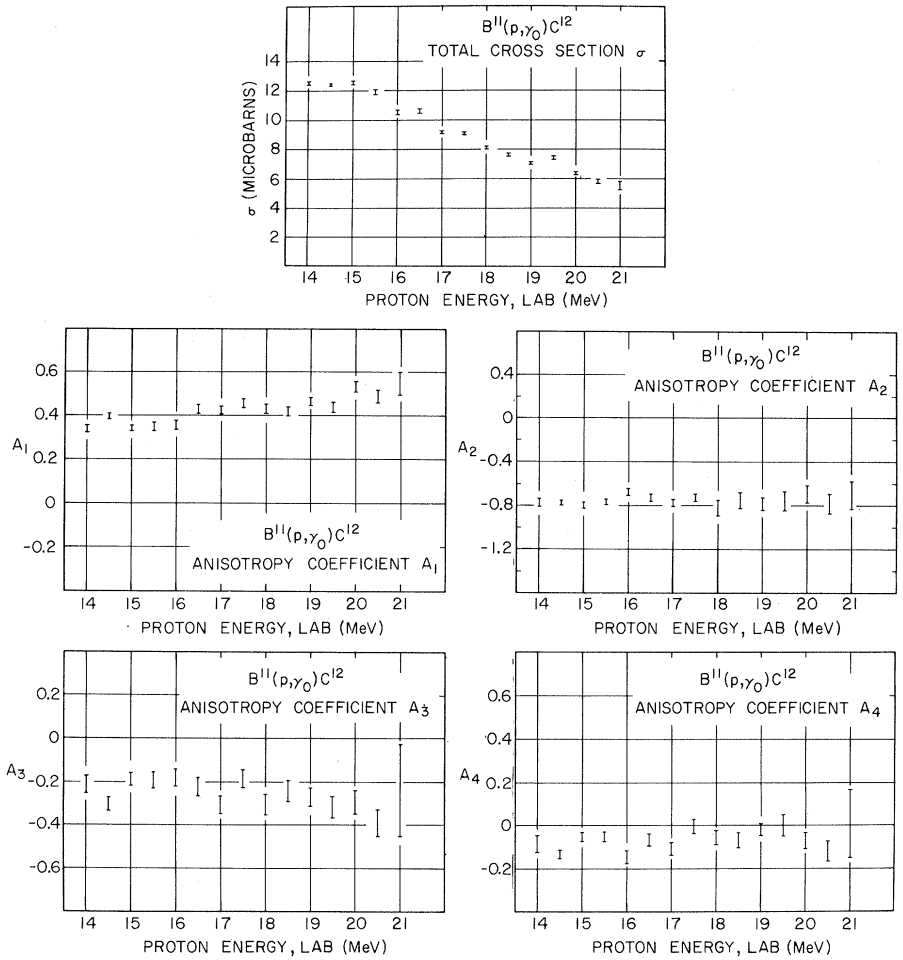

FIG. 11. Excitation functions for the total cross sections and angular-distribution coefficients for the γ_0 transition. The errors quoted here have a precise significance and are discussed in the text. The angular-distribution coefficients are as defined in the text (not as in Figs. 8–10).

is computationally simpler than is the coupled-channel approach and has been used exclusively in the calculations reported herein. It should perhaps be emphasized that R-matrix theory is quite general and that no assumptions are introduced concerning the nature of the reaction mechanism. Neither direct-reaction nor compound-nucleus formation are assumed and the calculations are thus expected to remain valid not only for these two extreme cases, but also in the interesting intermediate cases.

Unfortunately, it was not found feasible to carry out such an R-matrix calculation with reference to the available standard references. This reflects the fact that little attention has been paid in these references to the matter of phase; this phase question becomes of crucial importance in the present case where many overlapping compound resonances are involved. Our calculations have therefore been developed *ab initio* from basic quantum mechanics[19] and from knowledge of the appropriate electromagnetic multipole operators.[20] These detailed derivations are lengthy[5] and will not be reproduced here; they form the subject of a separate publication.[21]

In order to place the results presented herein in context, however, we include a brief discussion of how the various quantities which enter into these R-matrix calculations were obtained: These include channel radii, boundary-value parameters, and reduced-width amplitudes. We then summarize our computational scheme briefly.

The calculation has been limited to 1p-1h states and in consequence only nucleon channels are included. The nuclear S matrix was computed from the model wave functions of Gillet and Vinh-Mau and the scattering state of the system was obtained from it. Finally, the γ transition rates were calculated. The nuclear S matrix was obtained by inverting the sum of the R matrix and a

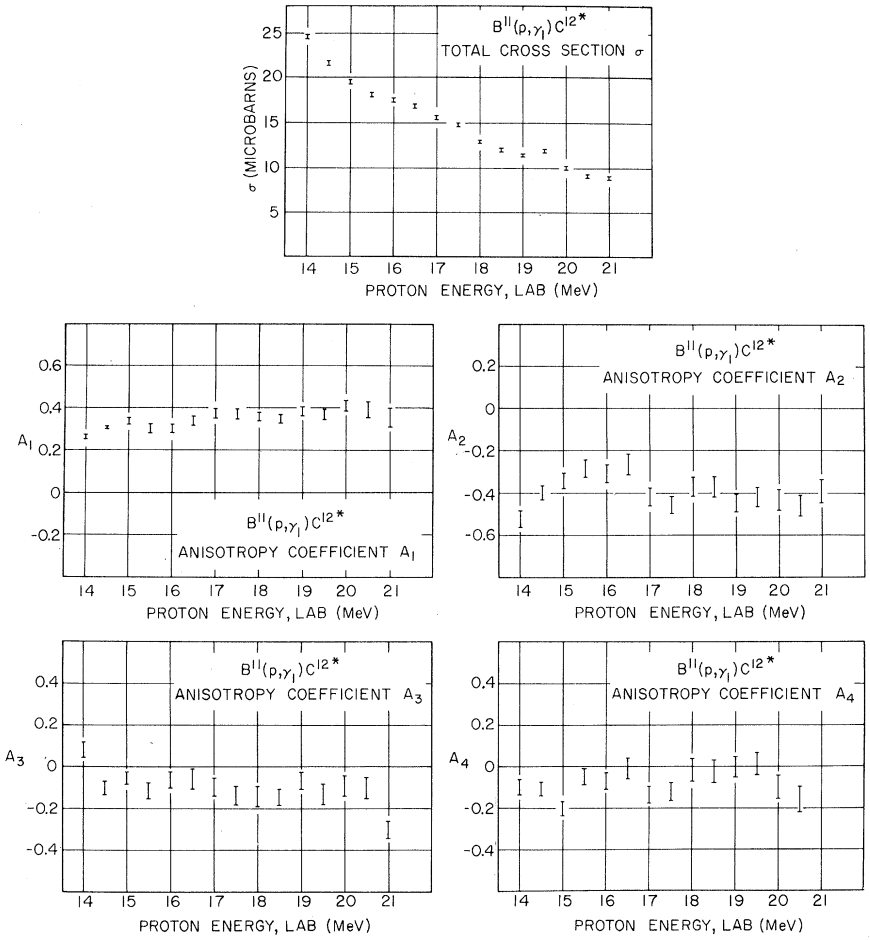

FIG. 12. Excitation functions for the total cross sections and angular-distribution coefficients for the γ_1 transition. The errors quoted here have a precise significance and are discussed in the text. The angular-distribution coefficients are as defined in the text (not as in Figs. 8–10).

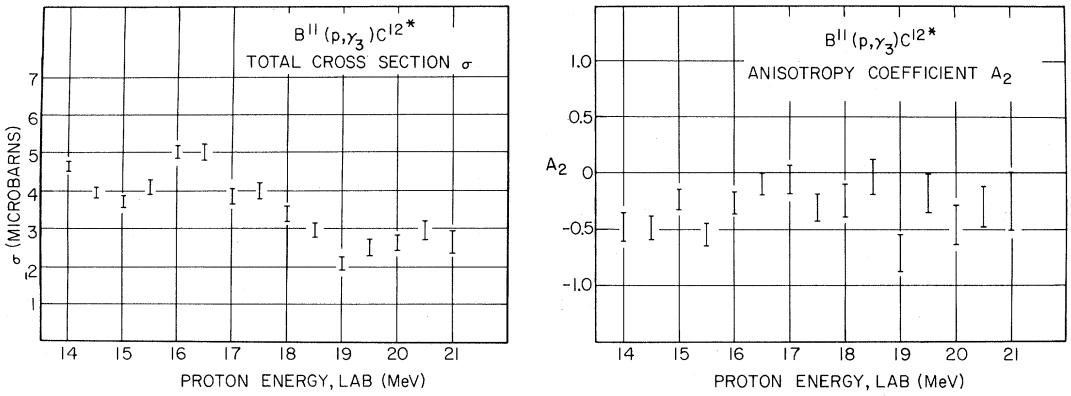

FIG. 13. Excitation functions for the total cross sections and angular-distribution coefficients for the γ_3 transition. The errors quoted here have a precise significance and are discussed in the text. The angular-distribution coefficients are as defined in the text (not as in Figs. 8–10).

diagonal channel matrix; use of the familiar many-level formula (which is invalid in this case) was thus avoided. The calculations involved all of the 64 states calculated by Gillet and 60 channels; it is perhaps worth noting that previous calculations have typically considered a very much smaller number of channels. Some of these channels, it must be emphasized, correspond to excited configurations in C^{11} and B^{11}. Physically, the importance of these configurations is more readily seen in the inverse photodisintegration reactions $C^{12}(\gamma,p)B^{11}$ or $C^{12}(\gamma,n)C^{11}$; clearly their effects are also present, however, in the reaction $B^{11}(p,\gamma)C^{12}$ in that they contribute additional width to the capture resonances.

The ground state of C^{12} arbitrarily has been taken as the particle-hole vacuum, in keeping with the Gillet assumptions. The ground states of C^{11} and B^{11} have been described as pure $1p_{3/2}$ holes in this vacuum. Although this is not necessarily in direct contradiction with the accepted view that the region of C^{12} is incorrectly described by pure j-j configurations, it is not expected to be a good approximation, and some discrepancies between prediction and experiment in the presently reported work are attributable to this oversimplification of the B^{11} ground state. We have not considered that the substantially greater effort which would have been required to include more realistic ground-state wave functions for B^{11} would be justified at the present time in view of the correspondingly crude approximations in the model under test. Our formalism[5] is, however, sufficiently general that such extensions are feasible.

In R-matrix theory, the channel radius should be chosen outside of the range of nuclear interactions but preferably as small as possible; a channel radius $R_c = 4.5$ F, based on the C^{12} experimentally determined nuclear-charge distribution[22] has been used in all our calculations. The boundary-condition parameters must be chosen to eliminate the Thomas-Ehrmann level shift for consistency with the work of Gillet which has been based on a fitting of the positions of the *observed* resonances; this is done by requiring that the logarithmic derivatives b_c of all the radial wave functions of relative motion be set equal to -1 at R_c.

The determination of the required nucleon reduced widths is more difficult, and we have not been able to avoid the introduction of a further

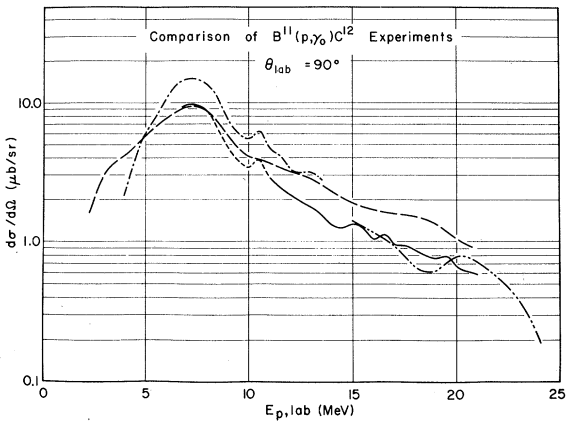

FIG. 14. Comparison of the data available on the $B^{11}(p,\gamma_0)C^{12}$ experiment. The cross section of Morrison (Ref. 12) (the long-dash line), obtained by detailed balance from $C^{12}(\gamma,p)B^{11}$ data taken with a bremsstrahlung beam, probably contains contributions from decays to excited states of C^{11} in the region above 10 MeV of proton energy. The data of RHL (Ref. 2) (the long-short-short-dash line) suffers from very large statistical errors. We are in disagreement with Allas *et al.* (Ref. 3) (the long-short-dash line) concerning the absolute magnitude of the total cross sections. Our results are indicated by the solid line with a short-dash section in the energy range 8 to 11 MeV.

parameter; fortunately, this parameter has limited influence on our predictions. For 1p-1h configurations with the hole in $1p_{3/2}$, the reduced widths were obtained from numerical integration of a realistic potential for C^{12}.[5,21] Such a potential – a modified Gaussian potential – is shown in Fig. 15. The parameters of the potential were obtained from electron scattering data,[22] with the exception of the potential depth, which was adjusted empirically to bind the $1p$ single-particle state by approximately 10 MeV, in accordance with the single-particle energies used by Gillet. The single-particle radial wave functions $u_{nl}(r)$ were numerically integrated, subject to the above boundary conditions in the case of the unbound states; Fig. 15 shows the nuclear potential for neutrons, while Fig. 16 shows the functions $ru_{nl}(r)$ for the neutron case. It should be noted that the unbound states exhibit a vanishing derivative of $ru_{nl}(r)$ at $r=R_c=4.5$ F, thereby satisfying the boundary conditions. The reduced-width amplitudes of the states with a hole in $1p_{3/2}$ and the particle in an unbound orbit ($1d$, $1f$, $2p$, or $2s$) are obtained directly by multiplying $u_{nl}(R_c)$ by the appropriate constant.

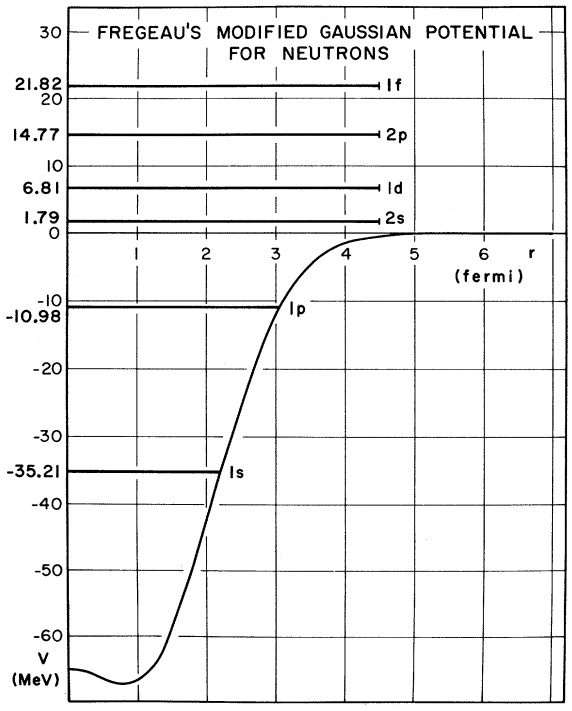

FIG. 15. The potential used for determining the neutron single-particle radial wave functions, from which the reduced widths were obtained. The single-particle eigenenergies are shown. The proton potential (not shown) was assumed to differ from the neutron potential simply by the Coulomb repulsion.

The configuration $(1p_{3/2})^{-1}(1p_{1/2})$ has a very low energy and its reduced width may be neglected. The reduced widths for configurations with a hole in the $1s$ shell must be discussed separately. Gillet predicts a state at 34-MeV excitation with an almost pure $(1s_{1/2})^{-1}(1p_{1/2})$ configuration; this particular configuration is bound, so that it has a vanishing reduced width. Calculations performed under such conditions have given rise to a very intense narrow resonance predicted at 34 MeV to correspond to this state. As found in our measurements, however, the resonance does not appear, contrary to the early work of RHL.[2] Gillet's prediction of this state at 34 MeV to consist of an almost pure $(1s_{1/2})^{-1}(1p_{1/2})$ configuration simply reflects the fact that numerous other configurations which exist in this energy region and higher, and which would mix with it, have not been taken into account in the calculation. These include many-particle–many-hole configurations and 1p-1h configurations of more than two-major-shell excitation. An adequate treatment of this problem is thus completely outside the scope of this work, but we have attempted to estimate the effect of the neglected configurations on the (p,γ) cross section for this state.

In the present discussion, it is simpler to focus on the inverse photonuclear reaction (γ,p), in which the C^{12} nucleus is excited to the $(1s_{1/2})^{-1}(1p_{1/2})$

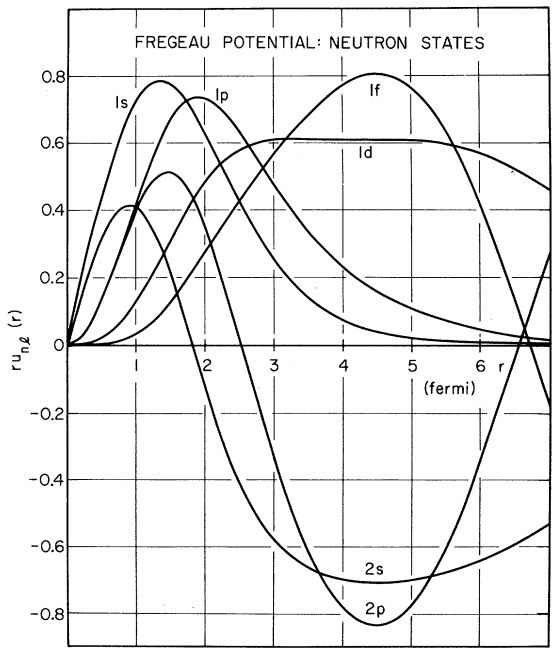

FIG. 16. r times the radial wave functions $u_{nl}(r)$ of the neutron single-particle states; they have been defined (for the unbound cases) be requiring a logarithmic derivative equal to -1 at $r=R_c=4.5$ F.

configuration by promoting a $1s$ particle to the $1p_{1/2}$ orbit. The underlying physical picture is that the $1p$ single-particle wave function represents an adequate approximation inside the nucleus, and that as soon as the $1p_{1/2}$ particle reaches the nuclear surface, its radial wave function resumes the oscillatory behavior characteristic of an open channel, instead of continuing to decay exponentially. Figure 17 shows qualitatively the uncorrected exponentially decaying $1p$ radial wave function and its corrected version with oscillatory behavior. It should be emphasized at this point that in a correct calculation these modifications in the tail of the $1p$ radial wave function would arise through the inclusion of many very small admixtures of 1p-1h configurations of many-shell excitation. These arguments also show the necessity for introducing such configurations in any more complete calculation; even though the low-lying states may contain only very small admixtures of them, their presence becomes important near the nuclear surface.

Two additional factors must be considered in estimating the reduced widths: Firstly, an enhancement factor of 9 is expected in the cross section, because there are nine $1p$ particles which can escape (the eight $1p_{3/2}$ particles must also be considered unbound in this framework), and second, the decay by emission of a $1p$ nucleon will not necessarily proceed through the B^{11} ground-state-plus-proton channel. This enhancement brings a factor of 3 to the reduced-width amplitudes, while the possibility of feeding other channels than the second state decreases the reduced-width amplitude by a factor which is difficult to estimate reliably; we have thus introduced a parameter ω which is defined through the expression:

$$\gamma = (0.427\ \mathrm{MeV}^{1/2})\omega ,$$

where 0.427 $\mathrm{MeV}^{1/2}$ is the value expected for the reduced-width amplitude on the basis of the uncorrected $1p$ radial wave function. Thus, ω is expected to be somewhat smaller than 3.0; we have performed our calculations with both $\omega = 2.8$ and $\omega = 1.0$.

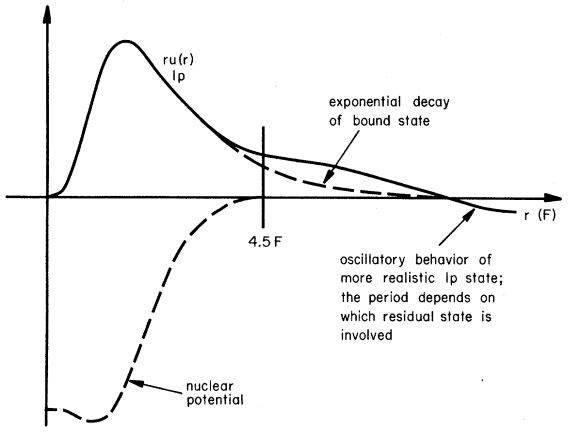

FIG. 17. This figure shows how the higher-order 1p-1h configurations neglected by Gillet were actually taken into account in evaluating the reduced width of the highly excited $(1s_{1/2})^{-1}(1p_{3/2})$ configuration.

The above discussion is based on the assumption that the $(1s_{1/2})^{-1}(1p_{3/2})$ configuration is mixed primarily with 1p-1h configurations of higher excitation; it may be mixed strongly with the many-particle–many-hole configurations, for example with the 3p-3h states[16]; this situation would produce a resonance around 34 MeV, in the (γ, h) cross section, instead of contributing to the (γ, p) cross section. Recent work in this laboratory by Shay *et al.*, to be published shortly,[23] indicates that a corresponding resonance is indeed present in the (h, γ) cross section.

The reduced-width amplitudes of the 1p-1h configurations in their corresponding channels are given in Table I; they are defined by the expression[24]:

$$\gamma = \hbar c_0 (2mc_0^2 R_c)^{-1/2} R_c u(R_c)$$

or

$$\gamma = (2.247\ \mathrm{MeV}^{1/2}) R_c u(R_c)$$

with the radial wave function $u(r)$ normalized according to

$$\int_0^{R_c} |ru(r)|^2 dr = 1 .$$

In these expressions m and R_c are the channel reduced mass and channel radius, respectively, and c_0 is the velocity of light. We have disregarded the slight difference between the proton and the neutron reduced widths, and have set the neutron

TABLE I. Absolute values of reduced-width amplitudes used in the calculation. These reduced widths were calculated according to the definition of Wigner; their signs are not quoted here, since the various phase conventions which make these signs meaningful have not been made explicit herein; they will be included in a further more complete publication.

Single-particle state	γ ($\mathrm{MeV}^{1/2}$)
$1p$	See text
$1d$	1.450
$1f$	1.850
$2s$	1.638
$2p$	1.883

TABLE II. Radial integrals for the $E1$ electromagnetic transition. The phase conventions used here assume a positive $u(r)$ for small values of r, as indicated in Fig. 15. u' reads across and u down.

$L=1$	$1s$	$1p$	$1d$	$1f$	$1s$	$2p$
$1s$		1.05				0.18
$1p$	1.05		1.41		−0.95	−1.32
$1d$		1.41		2.04		
$1f$			2.04			
$2s$		−0.95				1.76
$2p$	0.18		−1.32		1.76	

reduced widths equal to their proton counterparts.

Tables II and III contain the numerically integrated radial integrals for $E1$ and $E2$ transitions, respectively. These are defined as

$$\int_0^{R_c} u(r)u'(r)\left(\frac{r}{b}\right)^L r^2 dr\,,$$

where $u(r)$ and $u'(r)$ are the radial wave functions of the two single-particle states involved in the transition, and L is the transition multipolarity ($L=1$ or $L=2$). The values presented in Tables II and III are for proton transitions; the neutron integrals are not very different, and in consequence the proton radial integrals have been used for both proton and neutron transitions. The parameter b is a characteristic length introduced for proper dimensioning and has been arbitrarily chosen equal to 1.61 F.

In order to provide a more meaningful comparison between model prediction and experiment, the energies of the clearly identifiable model states were adjusted slightly to coincide with the observed resonances; it should be emphasized, however, that our calculations involve no free parameters other than the parameter ω, just introduced, which has limited influence and which, in any case, affects only the predicted 34-MeV resonance. In particular, the comparison of calculated and experimental absolute cross sections is meaningful, since no normalization of any sort has been performed in the calculations.

TABLE III. Radial integrals for the $E2$ electromagnetic transition. The phase conventions used here assume a positive $u(r)$ for small values of r, as indicated in Fig. 15. u' reads across and u down.

$L=2$	$1s$	$1p$	$1d$	$1f$	$2s$	$2p$
$1s$	1.11		1.37		−0.86	
$1p$		2.13		2.51		−1.25
$1d$	1.37		4.17		−4.10	
$1f$		2.51		5.10		−4.27
$2s$	−0.86		−4.10		4.40	
$2p$		−1.25		−4.27		4.40

Comparison of Model Predictions with Experiment

Figures 18–20 shows the comparison of these calculations with experiment; the data below 14-MeV incident proton energy 28.8-MeV excitation are from Allas *et al.*[3], except that the absolute magnitude of the total cross section was reduced to the value given by our more recent absolute cross-section measurements in this lower-energy range. Above this energy, the data are those reported herein. No data are presented for the A_1 and A_3 coefficients for the γ_3 transition, inasmuch as it was possible to fit the angular distributions successfully with only P_0 and P_2 Legendre polynomials. Figure 21 shows the contributions of the various incoming channels to the calculated cross sections.

Transitions to the C^{12} Ground State

Calculating the reduced widths of the 34-MeV 1^- state literally, i.e., taking the $(1s_{1/2})^{-1}(1p_{1/2})$ configuration as truly bound yields a narrow (1 MeV wide) compound-nucleus resonance of approximately 300-μb peak cross section, indicating that as noted above, the model wave function is not accurate enough near the nuclear surface to allow a direct extraction of the reduced widths in this case. When the reduced widths are calculated with the parameter ω introduced above, the resonance is still pronounced for $\omega=1$, but it has disappeared almost completely when the $1p$ reduced widths are increased by a factor of 3 ($\omega=3$). The fact that our measurements do not reveal the presence of a resonance in this region cannot, however, be interpreted as an unambiguous indication that these reduced widths are indeed large, since alternate explanations are possible; in particular, Rowe and Wong[25] predict that the $1s_{1/2}$ hole strength lies at higher energy, but it is more probable that this $[(s_{1/2})^{-1}(1p_{1/2})]_1$- configuration is mixed with several complex states which are not reached efficiently in the proton capture experiments. The apparent experimental resonance phenomena observed at 25 and 28 MeV (see Fig. 18) have such magnitude that they almost certainly involve electric dipole transitions, and should therefore be interpreted as resulting from interference of the transition amplitudes from these states with that of the main component of the giant resonance lying at 23 MeV. Although Gillet predicts a 1^-, $T=1$ state in this 25–28-MeV region, consisting primarily of the $(1p_{3/2})^{-1}(1d_{3/2})$ configuration, the resonances at 25 and 28 MeV remain unexplained in this context, because this predicted state contributes at most a negligible amount to the calculated cross section; furthermore, the

observed resonance is too narrow to be interpreted as originating from the $T=1$ admixture of a predominantly $T=0$ state. The only remaining explanation involves interpretation of these resonances as predominantly many-particle–many-hole states, with a substantial admixture of 1p-1h state through which they are populated and observed. We find, below, that the γ_1 cross section offers even more striking evidence for the participation of such many-particle–many-hole states.

It should be emphasized that we have been able to reach such conclusions only after having calculated the predicted excitation function in detail. When comparison is made only with the calculated transition strength for each individual model state, as has been customary in the past, it is easily possible to identify erroneously fine structure in the experimental excitation function with these individual states. This is particularly evident in the case of the γ_1 data where, lacking the detailed calculations, it might seem reasonable to identify the structure in the experimental data with the numerous one-particle–one-hole states involved in the capture; reference to our calculations, however, shows that the contributions from these states lead to no structure. We are thus led to conclude that observed structure reflects the participation in the capture of much more complex many-particle–many-hole configurations, which because of this complexity might be expected to have relatively narrow widths.

That a calculation such as that described here, which disregards many-particle–many-hole states, yields reasonable results for the γ_0 angular distri-

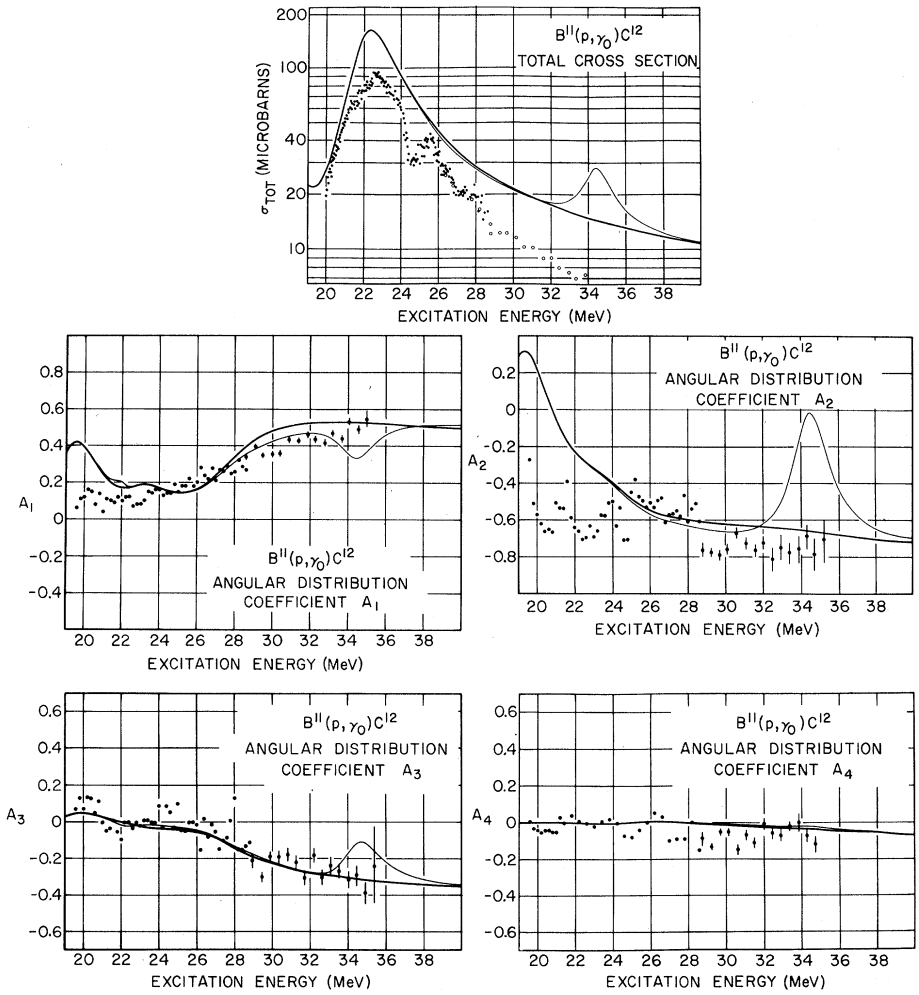

FIG. 18. Comparison of calculation obtained with Gillet's wave functions and the experimental results for the γ_0 transition. The plain dots are the results of Allas *et al.* (Ref. 3) with our normalization. The open circles and the dots with error bars are our data. The heavy line was obtained with $\omega=2.8$, whereas the faint line corresponds to $\omega=1.0$. The parameter ω is defined in the text, and *no other* free parameter is involved in the calculations.

butions must not be regarded as evidence for the purity of the 1p-1h states. Instead, the fact that the absolute cross section is predicted to be much larger than is observed experimentally (Figs. 18–20) suggests the presence of substantial admixtures of these configurations; Shakin and Wang[16] have shown, for example, that the admixture of 3p-3h configurations resulted in a substantial decrease of the calculated cross section.

The crude assumption that the ground state of B^{11} consists of a pure hole in $1p_{3/2}$ also leads to an overestimated cross section. The presence of an excited $\frac{3}{2}^-$ level near 5 MeV in C^{11} and B^{11} suggests that the ground states of these nuclei have many admixtures of other configurations; this view is in agreement with the various authors who have reported model wave functions for the B^{11} ground state.[26]

Transitions to the First Excited C^{12} State at 4.43 MeV

In the case of the γ_1 transition, the discrepancies between model prediction and experiment are much more pronounced, and the evidence for more complex configurations is more direct as we have noted above. In order to understand the γ_1 transition we consider the gedanken experiment of γ-ray absorption by an excited C^{12} target [in its first excited state, which is predominantly $(1p_{3/2})^{-1}(1p_{1/2})$]. As shown in Fig. 22, there is only one $1p_{1/2}$ particle, but seven $1p_{3/2}$ particles, which can be promoted by the γ absorption; we therefore expect to reach 1p-1h states with much less probability than 2p-2h states. The total γ-ray absorption might therefore be expected to be approximately 8 times more intense than a 1p-1h

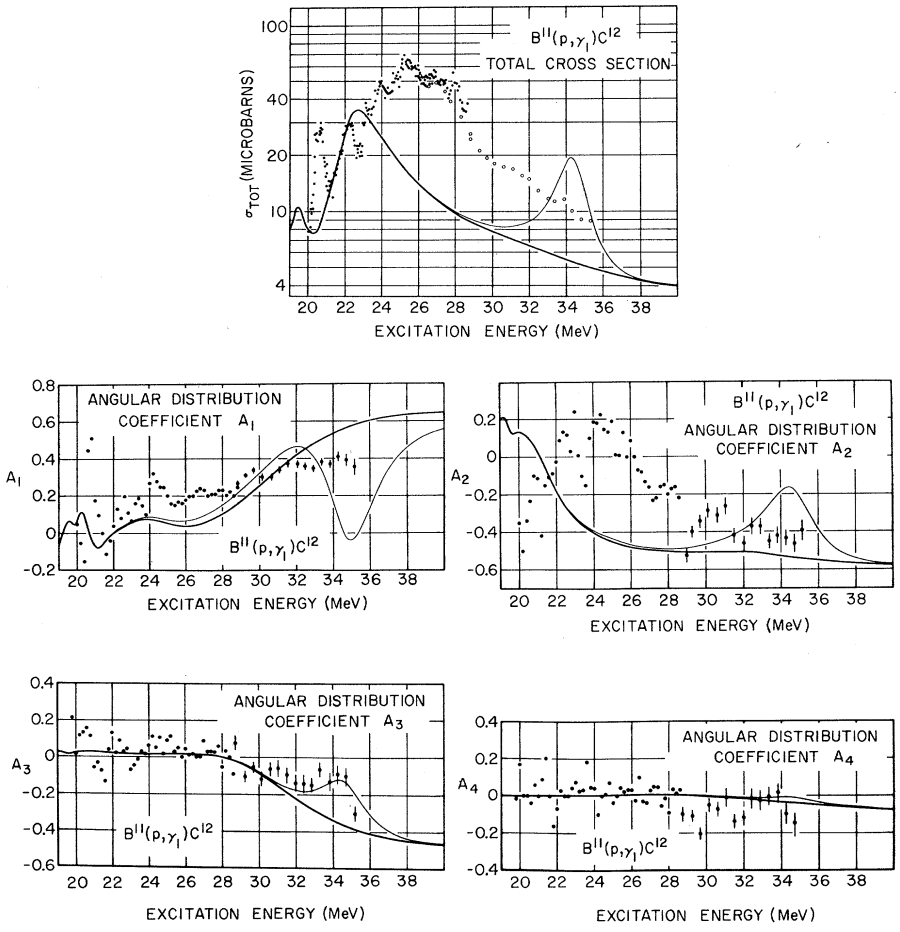

FIG. 19. Comparison of calculations obtained with Gillet's wave functions and the experimental results for the γ_1 transition. The plain dots are the results of Allas *et al.* (Ref. 3) with our normalization. The open circles and the dots with error bars are our data. The heavy line was obtained with $\omega = 2.8$, whereas the faint line corresponds to $\omega = 1.0$. This parameter ω is defined in the text, and *no other* free parameter is involved in the calculations.

model would have predicted. The (γ,p_0) cross section, which is of interest here, however, would not be enhanced by this factor of 8, because these 2p-2h states would decay primarily to excited states in B^{11}, reaching the ground state through its admixture of 1p-2h configurations. We nevertheless would expect a substantial net enhancement, since our γ_0 transition measurements discussed above have already indicated that the B^{11} ground state is far from being a pure hole in $1p_{3/2}$. The enhancement should be at an energy of approximately 4 MeV above the calculated 1p-1h contribution, taking into account the energy of the first excited state of C^{12}. The situation for (p,γ_1) we then obtain through detailed-balance arguments; we find experimentally that there *is* a substantial enhancement of the cross section, centered approximately 4 MeV above the calculated 1p-1h contribution. Drechsel, Seaborn, and Greiner[27] have

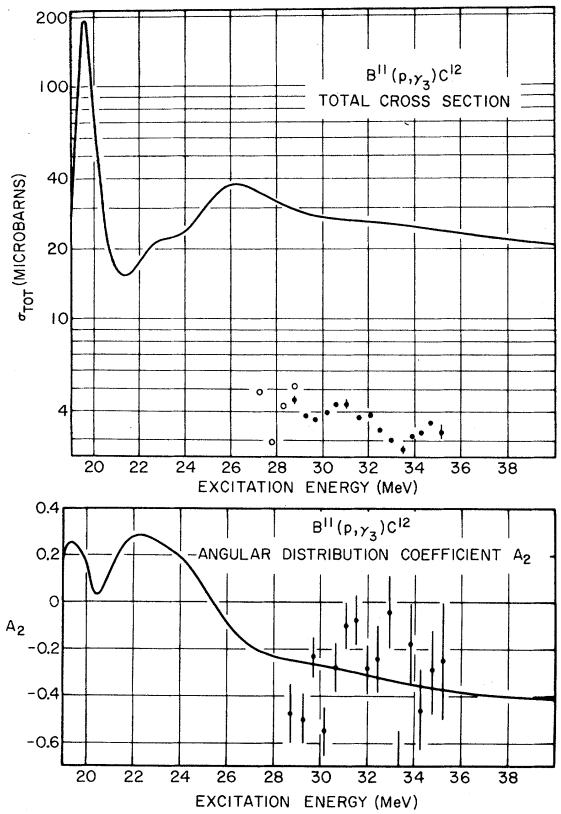

FIG. 20. Comparison of calculations obtained with Gillet's wave functions and the experimental results for the γ_3 transition. The plain dots are the results of Allas *et al.* (Ref. 3) with our normalization. The open circles and the dots with error bars are our data. The heavy line was obtained with $\omega=2.8$, whereas the faint line corresponds to $\omega=1.0$. This parameter ω is defined in the text, and *no other* free parameter is involved in the calculations.

calculated the (p,γ_0) cross sections, including certain collective effects (the coupling of the giant resonance with the low-energy vibrational models) and have obtained the otherwise missing strong transition around 25 MeV; unfortunately, they did not calculate cross sections, but only transition strengths, nor was a result presented for the (p,γ_1) transition, which would constitute an interesting test for such a model. Kamimura, Ikeda, and Arima[28] have developed a model in which the dipole oscillation and quadrupole vibration are coupled and have enjoyed success in predicting the positions and strengths of resonances seen in both $B^{11}(p,\gamma_0)C^{12}$ and $B^{11}(p,\gamma_1)C^{12}$. We believe that such approaches, qualitatively similar to the older idea of a giant resonance built on the first excited state, represent a promising direction.

Transitions to the Second Excited State of C^{12} at 7.66 MeV

As indicated above, we have seen no evidence for radiative capture leading to populations of this excited 0^+ state. This would be consistent with a relatively complex structure for this state as is indeed indicated also by its relatively strong population in helion capture experiments by Shay *et al.*[23]

Transitions to the Third Excited State of C^{12} at 9.65 MeV

For the transition to the third excited state, the situation is reversed: The calculated cross section is 10 times larger than measured. This suggests that the wave function given by Gillet for the 3^- third excited state is seriously deficient. This possibility has already been noted by Gillet[29] on the basis of the peculiar variation of the energy of the calculated level found as a function of the parameters of the residual interaction. The most reasonable interpretation appears to be that this 3^- state consists mainly of complex configurations, with only some 10% admixture of 1p-1h configurations through which most of the γ transition proceeds.

The low-energy resonance of the γ_3 transition shown at 19.5 MeV (3.8-MeV incident proton energy) in Fig. 20 is predicted as a strong $M1$ transition, from a 3^- level to the 9.64-MeV 3^- level. Such a 3^- to 3^- strong $M1$ transition has been reported by Feldman, Suffert, and Hanna,[30] at 2.6-MeV incident proton energy. Unfortunately, this lies below the neutron threshold, and to repeat our calculations with the correct resonance energy in order to allow a more direct comparison would have required extensive modifications to our programs. It is interesting to note that our

calculations predict an A_1 angular-distribution coefficient changing from positive to negative values as the energy is increased through the resonance, apparently in complete disagreement with the experimental results. We have no explanation for this behavior.

General Comments Concerning the Model Predictions

The calculated shape of the angular distributions for the γ_0 transition are in excellent agreement with the experimental data considering the absence of any useful fitting parameter. In particular, the fact that the measured angular distribution does not show any resonant behavior near the 25-MeV resonance constitutes evidence that this 25-MeV resonance proceeds through an admixture of the dominant $(1p_{3/2})^{-1}(1d_{5/2})$ configuration.

For the γ_1 transition, the angular distributions are not predicted nearly as well, reflecting increased importance of the higher-order configurations neglected in the calculations. For the γ_3 transition, the agreement is reasonable, but unfortunately the large experimental uncertainties do not permit a stringent test of the accuracy of the 1p-1h part of the wave function.

Figure 21 shows the calculated contributions of the various channels to the γ_0, γ_1, and γ_3 cross sections. The γ_0 transition is dominated by the $(1p_{3/2})^{-1}(1d_{5/2})$ configuration, while the 1p-1h contribution to the γ_1 transition arises mostly from the $(1p_{3/2})^{-1}(1d_{3/2})$ configurations, coupled to 3^-, 2^-, and 1^-, in that order of importance. The γ_3 total cross section is predicted to originate in the $[(1p_{3/2})^{-1}(1d_{5/2})]_{3^-}$ configuration (low-energy strong

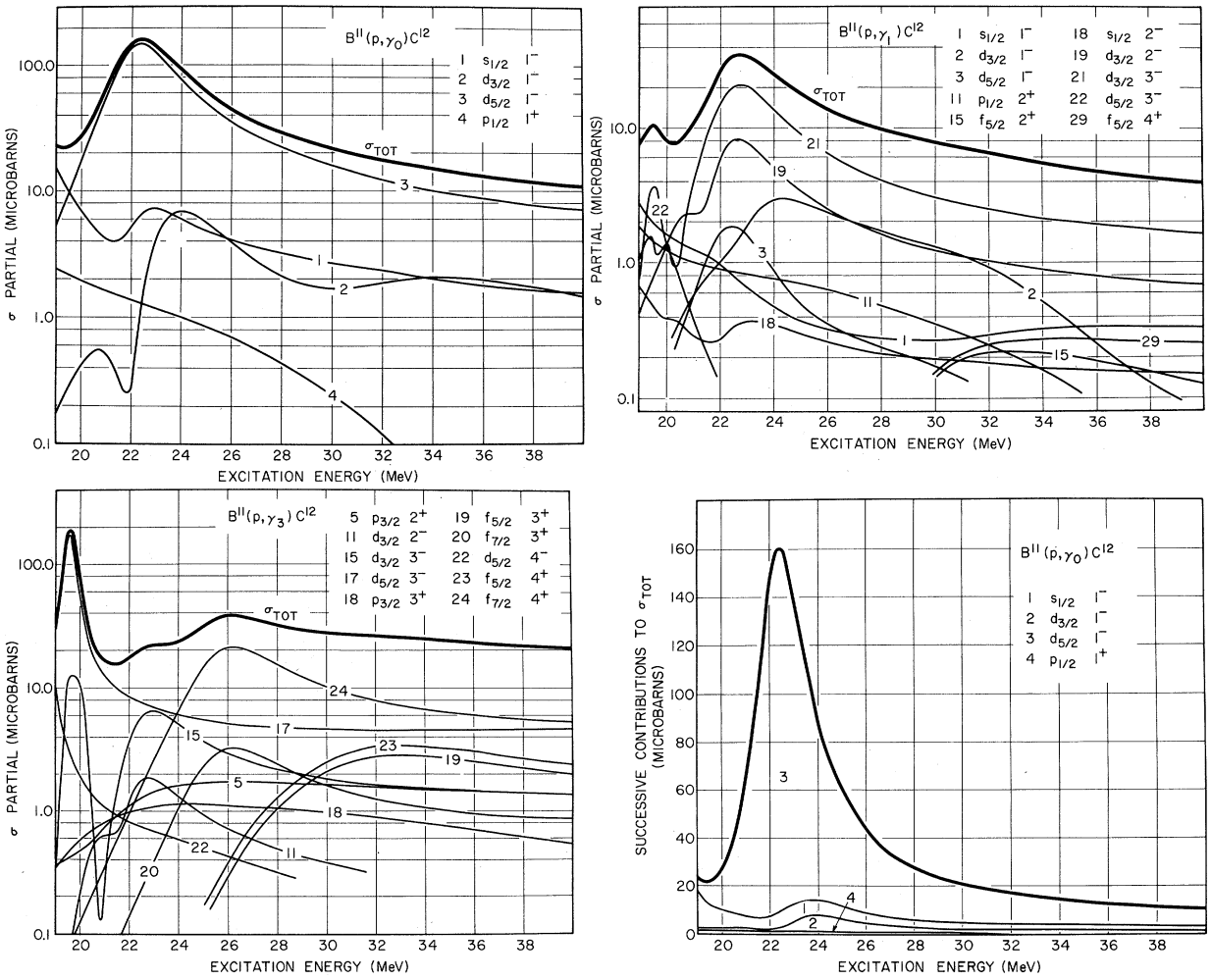

FIG. 21. Partial contributions from the various incoming channels to the γ_0, γ_1, and γ_3 calculated total cross sections. The γ_0 contributions are also shown on a linear scale to emphasize the dominance of the $[(1p_{3/2})^{-1}(1d_{5/2})]_{1^-}$ configurations over the entire energy range. The parameter ω defined in the text was set equal to 2.8 for these calculations.

$M1$ transitions) and in the $[(1p_{3/2})^{-1}(1f_{7/2})]_{4^+}$ configurations.

It is important to note that the structure present in the γ_1 total cross section *cannot* be explained in terms of the greater number of levels which can contribute an $E1$ transition to the first excited state (1^-, 2^-, and 3^- states contribute an $E1$ transition to the 2^+ first excited state, whereas only 1^- states can decay to the 0^+ ground state through an electric dipole transition). When comparing the measured cross sections with the set of discrete transitions calculated from a harmonic-oscillator-potential approach, it is tempting to relate the large number of experimentally observed maxima (i.e. resonances) with the equally large number of transitions which contribute to the total cross section. Figure 21, however, clearly shows that the widths of each of the contributing transitions is such that realistic calculations predict a cross section without appreciable structure. The structure present in the γ_1 total cross section, as well as the discrepancy in its absolute magnitude (which cannot be obtained from the point of view of discrete transitions), must be interpreted as direct evidence for the presence of more complex configurations.

Calculations with Pure *j-j* Configurations

Calculations of the γ_0 angular distributions were also performed using pure *j-j* configurations for the C^{12} wave functions and the same energies as above (i.e., the wave functions of Gillet were in each case replaced by their dominant configuration). This calculation was performed in the hope of demonstrating the importance of configuration mixing in C^{12}. It was performed with a value of the parameter ω equal to 1.0. The results are shown in Fig. 23. These are rather striking, in that there exists no appreciable difference between the cross sections predicted with Gillet's wave

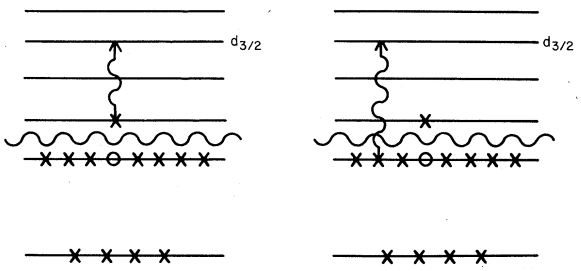

FIG. 22. Diagram of the $C^{12*}(\gamma_1,p_0)B^{11}$ gedanken experiment of photonuclear excitation of the C^{12} first excited state, explaining the enhancement in the inverse reaction studied herein. This enhancement proceeds through many-particle–many-hole states neglected by Gillet, and through the 1p-2h components of the B^{11} ground state.

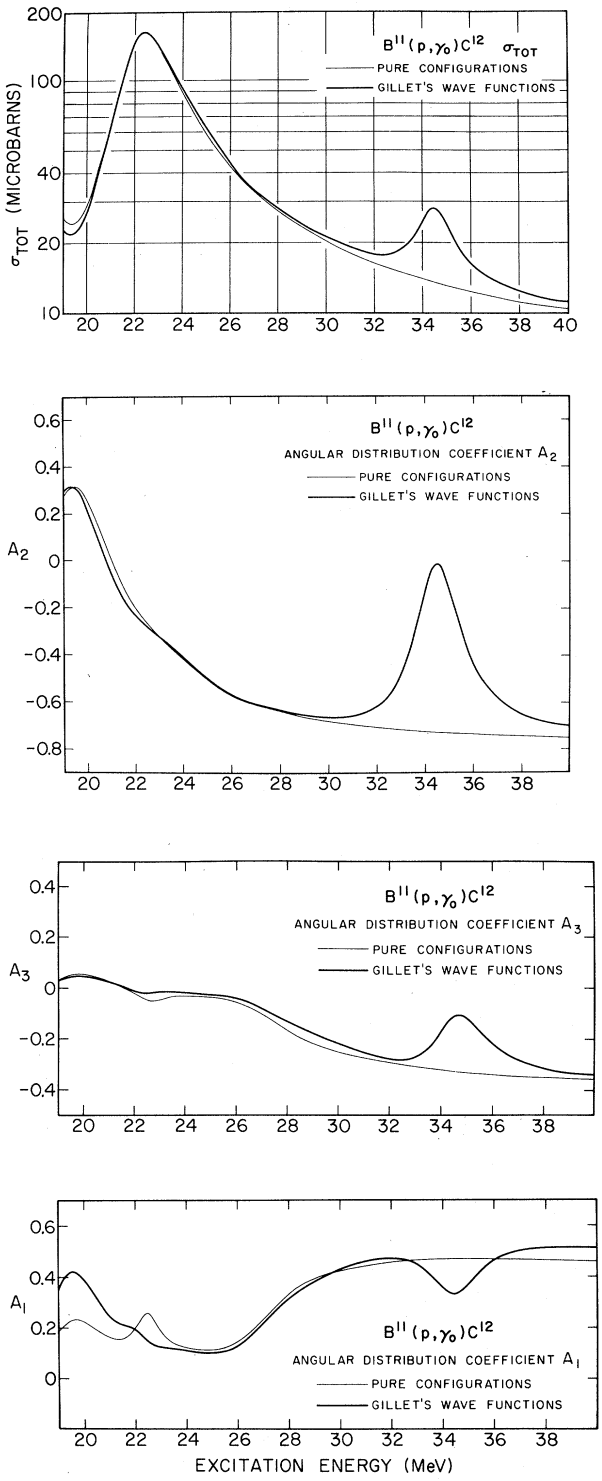

FIG. 23. Comparison of calculations based on Gillet's 1p-1h wave functions, with a similar calculation based on the more simple pure *j-j* configurations. The result based on the pure configurations is at least as good in reproducing the data as the Gillet wave functions have been. The calculations were performed with $\omega = 1.0$.

functions and those predicted with pure configurations, except for predictions concerning the unobserved 34-MeV resonance.

Among other results, it follows that the relative success of Gillet's wave functions in predicting the γ_0 angular distributions cannot be attributed to their detailed accuracy; this success is really that of R-matrix theory and pure j-j configurations. On the other hand, we must remark that Gillet's wave functions appear qualitatively correct in predicting little mixing of the j-j basis configurations. We have found it difficult to devise an experiment which would permit a verification of the accuracy of Gillet's wave functions in the region of the continuum, because the predicted admixtures are in general too small. (The 34-MeV state is an exception, but we have seen that in this case Gillet's wave functions give unreasonable results.)

It cannot be argued that, since Gillet fitted the C^{12} energies with reasonable success, the wave functions obtained through diagonalization of the residual interaction must be correct. The unperturbed energies were obtained from experiment and the level positions were fitted by an *ad hoc* residual interaction, and it thus seems best to think of it as a convenient parametrization leading to wave functions and residual interactions which do not necessarily have any precise, quantitative physical significance.

General Comments Concerning Particle-Hole Calculations

One of the major difficulties with all the nuclear structure p-h calculations using harmonic-oscillator wave functions and residual interactions is the necessity of introducing experimental energies for the unperturbed single-particle states. We suggest that this difficulty is directly related to the use of harmonic-oscillator potentials, and suggest how it may be alleviated for greater consistency. For the purpose of this demonstration we assume that the harmonic-oscillator potential provides a reasonable estimate of the nuclear potential well inside the nucleus, and represents the potential outside the nucleus by a constant (for neutrons) and a pure Coulomb field (for protons). The single-particle potential for neutrons is then represented in Fig. 15 where we have arbitrarily cut off the harmonic-oscillator potential while keeping the potential continuity. The interesting quantities are the logarithmic derivatives of the radial parts of the single-particle wave functions at R_c, the cutoff radius. These numbers are easily obtained and range typically from −4 to +2. The condition for a vanishing level shift is that the logarithmic derivatives be equal to −1, as we have noted above. This condition is clearly not met by the harmonic-oscillator wave functions, and it is interesting to compute the actual Thomas-Ehrmann level shifts resulting from the large logarithmic derivatives. These level shifts arise automatically in the matrix-inversion procedure used in the presently reported calculations, and they range from −6 to +6 MeV, typically, in the energy region under consideration. In other words, two states at the same energy can produce resonances 12 MeV apart, and inversely. This fact has not been given adequate recognition and the level shifts are often completely disregarded in the literature when using harmonic-oscillator wave functions.

This also illustrates clearly why the experimental energies (which already contain level shifts) had to be introduced. In order to alleviate this problem, it is easy to introduce a realistic potential in place of the harmonic-oscillator potential, and to define the eigenstates and eigenenergies through the appropriate boundary condition; a spin-orbit potential is then introduced to split the configurations corresponding to the same l. Finally, the radial matrix elements are obtained numerically. We believe that a particle-hole calculation would not only gain in consistency through the above procedure, but also that the residual interactions obtained through the fitting of level positions would become more meaningful.

Another remark of general applicability concerns the use of a truncated basis in calculating particle-hole wave functions of nuclear states. The effects of disregarding all many-particle–many-hole configurations and of retaining only two-major-shell or less excitations (n, l truncation) have been discussed above; in particular, this leads to an almost pure $[(1s_{1/2})^{-1}(1p_{1/2})]_1$-

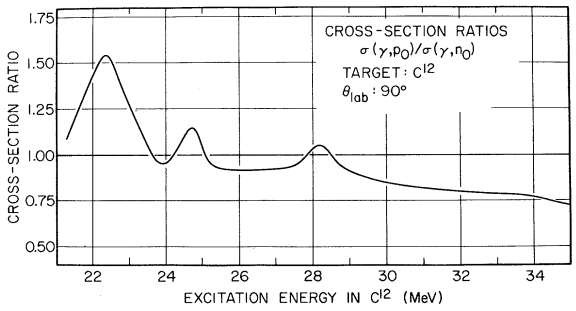

FIG. 24. Ratio of 90° differential cross sections C^{12}-$(\gamma,p_0)B^{11}$ and $C^{12}(\gamma,n_0)C^{11}$. Above 28 MeV, the (γ,p_0) cross sections have been obtained by detailed balance from our (p,γ_0) data; below 28 MeV, by detailed balance from the data of Allas *et al.*, normalization to our results in the region of overlap. The (γ,n_0) cross sections are the data of Wu *et al.* (Ref. 33).

configuration at 34-MeV excitation. This state, taken literally, is particle bound, since the $1s$ and $1p$ particles are bound; we see that a reasonable eigenstate will in fact be mixed with a large number of small components of higher-n configurations which have a larger value near the nuclear surface, thereby modifying the radial wave function in the corresponding $1p_{1/2}$ channel near the channel surface, and permitting the state to decay. In other words, the nuclear reaction will proceed through small admixtures of higher-n configurations which are important near the channel surface and which have been neglected from the start by the truncation of the basis.

This reasoning implies that substantial amounts to many-particle–many-hole configurations found as admixtures of predominantly simpler states (the ground states of C^{12} and O^{16} for example) may arise spuriously in calculations which use n, l truncated basis, in order to explain reactions which in fact proceed through higher-n configurations.

If a nuclear-structure calculation were to be performed with a complete basis X, and a similar calculation be repeated with a subset x of X, we should not expect that the resulting wave functions will have a large overlap. This is because the truncated basis x is attempting to correct for the missing configurations by modifying the admixtures of these configurations which it contains. The net result is to decrease the overlap between the states calculated with x and those calculated with X, while in a restricted sense making them more similar. The end result is that while the wave functions calculated with x may be completely unphysical, they may still lead to very reasonable results for most observables calculated with them.

V. ISOSPIN MIXING IN C^{12}

As is now well known[31,32] comparison of the cross sections of the reactions $C^{12}(\gamma,p_0)B^{11}$ and $C^{12}(\gamma,n_0)C^{11}$ can lead to an estimate of the degree of isospin mixing in giant-resonance states. Figure 24 shows the ratio of (γ,p_0) to (γ,n_0) 90° cross sections. The (γ,n) data are taken from Wu[31]; below 28-MeV excitation, the (γ,p_0) results are computed via detailed balance from Allas's (p,γ_0) results, renormalized to our more recent measurements; above 28 MeV, the (γ,p_0) cross sections are from the data presented herein.

Figure 25 is a plot of the ratio α_0/α_1, where α_0 and α_1 are the amplitudes of the $T=0$ and $T=1$ configurations in the wave function of the excited

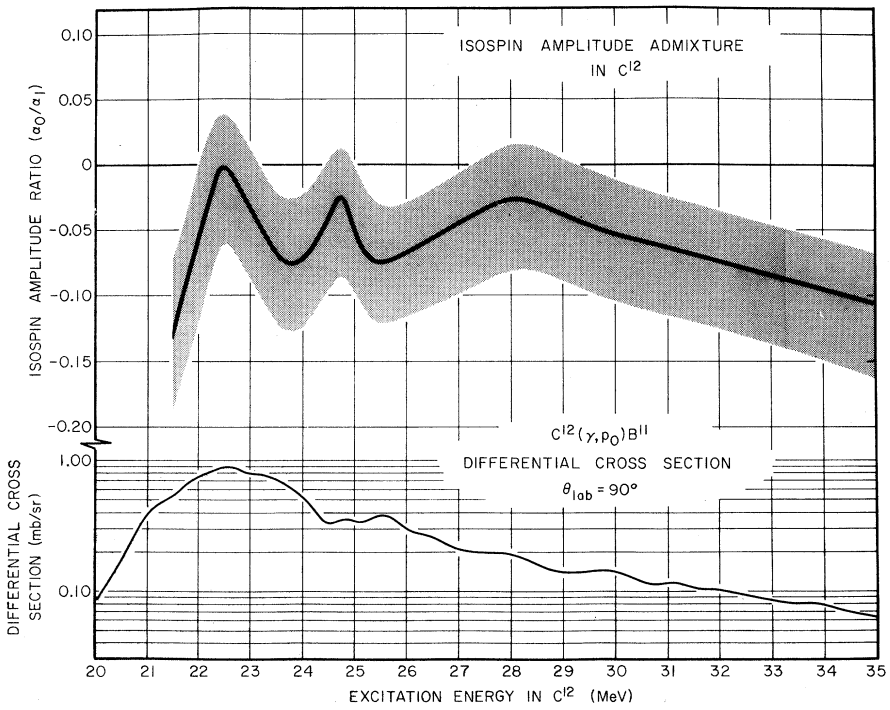

FIG. 25. The isospin amplitude mixing ratio (heavy line) has been estimated by applying the Barker-Mann expression to ratio $\sigma(\gamma,p_0)/\sigma(\gamma,n_0)$ shown in Fig. 24. The shaded region represents the limits determined by assuming a systematic uncertainty in our absolute cross sections of 20%.

state of C^{12}. The Barker and Mann relation[32]

$$\frac{\sigma(\gamma,p_0)}{\sigma(\gamma,n_0)}=\frac{P_p}{P_n}\left|\frac{\alpha_0+\alpha_1}{\alpha_1-\alpha_0}\right|^2,$$

where P_p and P_n are the proton and neutron penetrabilities, respectively, was used, and it was assumed that only the d-wave nucleon channels contribute to the transition. This last assumption is consistent with the results of our calculations; for example, see Fig. 21. The shaded area represents the limits imposed by the estimated systematic uncertainty in our absolute cross sections only, without any consideration of the additional uncertainty implied by possible systematic errors in the (γ,n_0) data of Wu *et al.*[33]

Once the possible systematic errors in $\sigma(\gamma,n_0)$ are included, Fig. 25 is not inconsistent with an over-all negligible isospin mixing, except at the resonances. The drop in α_0/α_1 at high energy may be incorrect, since a small contribution from the decay to excited states of C^{11} in the nominally (γ,n_0) results would suffice to produce this effect. The bremsstrahlung end points chosen by Wu are such that a small contribution from the transitions to excited states cannot *a priori* be ruled out.

On the basis of the cross sections reported here the isospin mixing in the giant-resonance region of C^{12} is thus found to be rather small and similar to that in O^{16} as reported by Wu *et al.*[33]

VI. CONCLUSION

A number of results of general applicability have been obtained: From the experimental point of view, we have found that the previously published $B^{11}(p,\gamma)C^{12}$ absolute cross sections are open to some question. From the theoretical point of view, we have demonstrated that the necessity of introducing experimental energies in particle-hole calculations is linked with the use of the harmonic-oscillator potential. A method for calculating (p,γ) cross sections and angular distributions has been developed, based on R-matrix theory, and reduced widths have been calculated consistently. It has been shown that radiative capture experiments, and particularly those transitions leading to excited states can provide rather detailed structure information.

Other results are more specifically applicable to our understanding of C^{12}. It has been found that the (p,γ) cross sections and angular distributions are reasonably described by the 1p-1h model with pure j-j configurations and pure isospin, the discrepancies being attributable to the mixture of more complex configurations.

The discrepancy in the prediction of the absolute magnitude of the γ_0 cross section is meaningful and is interpretable as arising partly from the oversimplification of the B^{11} ground-state wave function and partly from the neglect of many-particle–many-hole configurations.

When all systematic errors are taken into account, the (γ,n) and (p,γ) data comparison (through detailed balance) appear consistent with essentially zero isospin mixing at high excitation energies in C^{12}, in agreement with observations in O^{16} but in contrast to the earlier reports for C^{12} which were based on different (p,γ_0) absolute cross sections. However, the isospin mixing certainly undergoes modification when the proton energy is varied through the capture resonances.

The calculations indicate that approximately 50% of the γ_1 transition strength originates in 1p-1h states, while the other half, centered at a somewhat higher energy, comes from 2p-2h configurations mostly, in accordance with the view of a giant resonance based on the first excited state of C^{12}.

The $[(1p_{3/2})^{-1}(1d_{5/2})]_1$- configuration completely dominates the γ_0 giant resonance in C^{12}; the 1p-1h part of the γ_1 transition is dominated by the three $(1p_{3/2})^{-1}(1d_{3/2})$ configurations.

Finally, the mixing of 1p-1h configurations represented by Gillet's wave functions does not improve the results; in fact, the pure j-j configurations yield slightly better results. The 34-MeV state predicted by Gillet, which should give rise to a large resonance according to his wave functions, does not appear in the experimental data. Subsequent to the work reported herein, Shay *et al.* in this laboratory have completed complementary studies on $Be^9(h,\gamma)C^{12}$ and $B^{10}(d,\gamma)C^{12}$ as well as a parallel set of measurements leading to O^{16}. These results will be published shortly.

ACKNOWLEDGMENTS

We are greatly indebted to H. Duncan, presently a graduate student at Massachusetts Institute of Technology, for his major contribution to the theory and computer programming underlying the calculations presented herein; these will be published separately. M. W. Sachs has contributed to the data-acquisition and -analysis phases of this work. W. Thompson has kindly supplied the B^{11} targets used in the determination of the absolute cross sections and has carefully examined the contaminants. Various members of the A. W. Wright Nuclear Structure Laboratory staff have collaborated with us on occasion; among them we particularly mention A. A. Aponick, R. Siemssen, and C. Maguire. Discussions with F. W. K. Firk were greatly appreciated. One of the authors (C.B.) wishes to thank the University of Montreal for its generous support throughout his graduate program.

†Work supported in part under U. S. Atomic Energy Commission Contract No. AT(30-1)-3223.

*Present address: DPh N/ME, C. E. N. de Saclay, 91 Gif-sur-Yvette, France.

‡Present address: Laboratoire de Physique Nucleaire, BP 20 CR, 67 Strasbourg, France.

§Present address: Physics Department, State University of New York, Albany, New York.

[1]H. E. Gove, A. E. Litherland, and R. Batchelor, Nucl. Phys. 26, 480 (1961).

[2]N. W. Reay, N. M. Hintz, and L. L. Lee, Jr., Nucl. Phys. 44, 338 (1963).

[3]R. G. Allas, S. S. Hanna, L. Meyer-Schützmeister, and R. E. Segel, Nucl. Phys. 58, 122 (1964).

[4]G. Kernel and W. M. Mason, Nucl. Phys. A123, 205 (1969).

[5]C. Brassard, Ph.D. thesis, Yale University, 1970 (unpublished).

[6]V. Gillet, Ph.D. thesis, Universite de Paris, 1962 (unpublished).

[7]V. Gillet and N. Vinh-Mau, Nucl. Phys. 54, 321 (1964).

[8]We are greatly indebted to Dr. J. Gibbons of the Oak Ridge National Laboratory for making this loan possible.

[9]C. Brassard, Nucl. Instr. Methods 94, 301 (1971).

[10]C. Brassard, to be published.

[11]J. Kockum and N. Starfelt, Nucl. Instr. Methods 4, 171 (1959).

[12]R. L. Bramblett, S. C. Fultz, B. L. Berman, M. A. Kelly, J. T. Caldwell, and D. C. Sutton, UCRL Report No. 70582, 1967 (unpublished).

[13]M. Suffert, W. Feldman, J. Mahieux, and S. S. Hanna, Nucl. Instr. Methods 63, 1 (1968); E. M. Diener, J. F. Amann, S. L. Blatt, and P. Paul, Nucl. Instr. Methods 83, 109 (1970).

[14]E. D. Earle and N. W. Tanner, Nucl. Phys. A95, 241 (1967); J. L. Black, W. J. O'Connell, S. S. Hanna, and G. L. Latshaw, Phys. Letters 25B, 405 (1967).

[15]R. C. Morrison, Ph.D. thesis, Yale University, 1966 (unpublished).

[16]C. M. Shakin and W. L. Wang, Phys. Rev. Letters 26, 902 (1971); H. Feshbach, Spring Meeting of American Physical Society in Washington (1971).

[17]M. Marangoni and A. M. Saruis, Nucl. Phys. A132, 649 (1969).

[18]E. Boeker and C. C. Jonker, Phys. Letters 6, 80 (1963).

[19]A. Messiah, Mecanique Quantique (Paris, France: DUNOD, 1962) [transl.: Quantum Mechanics (North-Holland, Amsterdam, 1965)].

[20]H. J. Rose and D. M. Brink, Rev. Mod. Phys. 39, 306 (1967).

[21]C. Brassard and H. Duncan, to be published.

[22]J. Frégeau, Phys. Rev. 104, 225 (1956).

[23]H. D. Shay, J. Long, R. Peschel, and D. A. Bromley, to be published.

[24]The signs of reduced-width amplitudes are extremely important; the incorrect results of the otherwise very interesting paper by Boeker and Jonker (Ref. 18) may be traced back to a slight error in these signs. The signs depend on several phase conventions, and since they would be meaningless without explicit description of all phase conventions, only the absolute values are presented herein; the more complete discussions of the calculations will (Ref. 5, 21) include an explicit description of the signs of the reduced-width amplitudes.

[25]D. J. Rowe and S. S. M. Wong, Phys. Letters 30B, 147, 150 (1969).

[26]A. N. Boyarkina, Izv. Akad. Nauk SSSR, Ser. Fiz. 28, 337 (1964) [transl.: Bull. Acad. Sci. USSR, Phys. Ser. 28, 255, (1964)].

[27]D. Drechsel, J. B. Seaborn, and W. Greiner, Phys. Rev. 162, 983 (1967).

[28]M. Kamimura, K. Ikeda, and A. Arima, Nucl. Phys. A95, 129 (1967).

[29]Gillet, Ref. 6, p. 150.

[30]W. Feldman, M. Suffert, and S. S. Hanna, Progress Report, January 1, 1967–January 31, 1968, Nuclear Structure Investigations with a FN Tandem Accelerator, Stanford University (unpublished), p. 12.

[31]C. P. Wu, Ph.D. thesis, Yale University, 1968 (unpublished).

[32]F. C. Barker and A. K. Mann, Phil. Mag. 2, 5 (1957).

[33]C. P. Wu, F. W. K. Firk, and T. W. Phillips, Phys. Rev. Letters 20, 1182 (1968).